Neuropsychiatric Disease and Treatment

Dovepress
Taylor & Francis Group

Open Access Full Text Article

CLINICAL TRIAL REPORT

Altered Effective Connectivity Within the Frontoparietal Network in Alzheimer's Disease and Its Modulation by Acupuncture: A Resting-State *f*MRI Study

Yu-Ting Wei[1,2,*], Li Li[1,*], Wen-Ting Xie[1], Yan Wang[1], Ya-Ru Zhao[1], Ren-Zhen Zhang[1], Ling Ma[1], Xing-Ke Yan[1,2]

[1]College of Acupuncture-Moxibustion and Tuina, Gansu University of Chinese Medicine, Lanzhou, Gansu, People's Republic of China; [2]Research Center of Traditional Chinese Medicine, Lanzhou, Gansu, People's Republic of China

*These authors have contributed equally to this work

Correspondence: Xing-Ke Yan, College of Acupuncture-Moxibustion and Tuina, Gansu University of Chinese Medicine, 35 Dingxi East Road, Lanzhou, Gansu, People's Republic of China, Email yanxingke@126.com

Purpose: Alzheimer's disease (AD) is increasingly prevalent, yet how acupuncture modulates cognitive brain networks remains unclear. We used resting-state *f*MRI (rs-*f*MRI) to examine whether acupuncture prescription regulates effective connectivity within the frontoparietal network (FPN) in AD.

Patients and Methods: Sixty AD patients were randomized to donepezil alone (drug group) or acupuncture plus donepezil (acupuncture group) for 6 weeks (n=30/group). Seven healthy controls were scanned once. Global cognition was assessed with MoCA-B. Independent component analysis identified the FPN, and Granger causality analysis quantified directed effective connectivity before and after treatment.

Results: Both interventions improved MoCA-B ($P<0.05$), with larger gains in the acupuncture group ($P<0.05$). Relative to controls, AD showed FPN disruption with compensatory reorganization. Decreased connectivity was observed from the left middle temporal gyrus (MTG) to the right inferior parietal lobule (IPL), and from the left median cingulate/paracingulate gyri ($P<0.05$). Increased connectivity emerged from the right IPL and left cingulate/paracingulate to the left MTG, and from the right IPL to the left medial frontal gyrus (orbital part) ($P<0.05$). The right IPL and left MTG were core FPN nodes. Post-treatment, the drug group showed reduced right IPL→left orbital medial frontal connectivity, whereas the acupuncture group showed reduced right IPL→left MTG connectivity ($P<0.05$). Between-group comparisons indicated acupuncture-specific modulation of right insula→left MTG and left precuneus→left MTG connectivity ($P<0.05$).

Conclusion: Acupuncture combined with donepezil provides superior cognitive benefits and selectively reshapes directed FPN interactions, supporting a network-level mechanism involving frontal–parietal–temporal integration.

Keywords: Alzheimer's disease, acupuncture, resting-state functional magnetic resonance imaging, frontoparietal network, effective connectivity

Introduction

Alzheimer's disease (AD) is a common neurodegenerative disorder in older adults.[1] Clinically, it is characterized by progressive cognitive decline, impaired activities of daily living, and behavioral and psychological disturbances.[2] Epidemiological studies indicate a strong association between AD onset and aging: the prevalence of AD is approximately 10% among individuals aged 65–75 years and increases to 32% in those over 80 years.[3] As of 2018, the number of people living with AD worldwide had reached nearly 50 million.[4–6] The continuous progression of AD compromises functional independence in older adults, leading to substantial impairment in self-care abilities and imposing a heavy economic burden on families and society. Consequently, AD has become a major public health challenge requiring urgent attention.[7,8]

https://doi.org/10.2147/NDT.S601136
Received: 4 February 2026
Accepted: 29 April 2026
Published: 13 June 2026

Current therapeutic approaches for AD include pharmacological treatment,[9] cognitive stimulation therapy,[10,11] and neuromodulation-based interventions.[12,13] Although these approaches can partially improve cognitive function, their limitations—such as adverse effects and the need for long-term administration—remain significant. In contrast, acupuncture is considered particularly effective for disorders related to cognitive dysfunction. Clinical and experimental evidence has shown that acupuncture produces notable therapeutic benefits in AD, offering advantages such as high patient adherence, good tolerability, and minimal side effects.[14] Moreover, the cognitive-enhancing effects of acupuncture in AD have been linked to multiple molecular mechanisms, such as regulating Aβ and tau protein expression, suppressing central inflammatory responses and oxidative stress, improving regional brain energy metabolism, enhancing synaptic plasticity, and modulating autophagy and neuronal apoptosis.[15]

Neuroimaging studies have revealed that multiple spatially distinct brain regions exhibit temporally synchronized low-frequency oscillations during rest, cooperating to regulate specific functional processes. These interconnected regions collectively form intrinsic functional brain networks.[16] Current research demonstrates that several cognitive domains impaired in AD—including episodic memory, executive function, attention, visuospatial orientation, and language—are regulated by key networks such as the default mode network (DMN), frontoparietal network (FPN), and attention network (AN).[17] Among these, the FPN serves as a central regulatory hub, dynamically integrating task demands and expected outcomes. It flexibly couples with task-related networks and modulates patterns and strengths of functional connectivity to support cognitive control.[18] Thus, we hypothesize that the FPN is a core network affected in AD and that its dysfunction is closely associated with disease progression.

Resting-state functional magnetic resonance imaging (rs-*f*MRI), based on the blood oxygen level-dependent (BOLD) mechanism of neurovascular coupling,[19,20] enables the monitoring of hemodynamic fluctuations associated with spontaneous neuronal activity and thereby provides an indirect but powerful method for assessing intrinsic brain function.[21] This technology offers valuable support for investigating the neural mechanisms underlying cognitive, behavioral, and psychological impairments in AD, as well as for elucidating the brain mechanisms of acupuncture. Granger causality analysis (GCA), which assesses directional causal relationships among rs-*f*MRI time series, allows the evaluation of cooperative interactions among different brain regions or networks and tracks the directional flow of information between them. As such, GCA is an effective tool for characterizing effective connectivity and understanding patterns of directional network interactions.[22]

However, few studies have examined whether acupuncture can modulate abnormal causal interactions within the FPN in AD. Therefore, in this study, we extracted the component regions of the FPN using independent component analysis (ICA) and applied bivariate granger causality modeling to assess causal relationships within the FPN in AD patients. We first compared effective connectivity patterns between AD patients (AD group) and healthy controls (HC group); subsequently, we analyzed the effects of donepezil hydrochloride and acupuncture on FPN effective connectivity in AD.

Materials and Methods

Study Design and Participants

This randomized controlled study was approved by the ethics committee of the Affiliated Hospital of Gansu University of Chinese Medicine (Approval No. [2022] 12). The study protocol was registered with the Chinese Clinical Trial Registry (ChiCTR2200056137) and conducted in accordance with the principles of the Declaration of Helsinki. All participants were fully informed of the study details, provided their voluntary consent to participate in this trial, and signed an informed consent form, which explicitly stated that they might undergo rs-*f*MRI scans. A total of 67 individuals were recruited between July 2021 and October 2022 from the Affiliated Hospital of Gansu University of Chinese Medicine, as well as through community advertisements (Before January 6, 2022, only basic information of potential participants who expressed willingness to participate was recorded; these individuals were not formally enrolled in the study. The present study officially commenced only after approval was obtained from the Ethics Committee). The sample consisted of 60 patients with AD (AD group) and 7 healthy controls (HC group) matched for age, gender, and educational level.

The 60 AD patients were randomly assigned to either the drug group or the acupuncture group (30 participants in each group) using random numbers generated by SPSS version 26. During the clinical evaluation phase, 2 participants in

the drug group were excluded due to adverse drug reactions, and 3 participants in the acupuncture group were excluded due to intolerance to treatment. For the neuroimaging component, among the volunteers who met the criteria for fMRI scanning, 15 participants were randomly selected for the scan using a computer-generated randomization sequence created with SPSS version 26. During data preprocessing, datasets were excluded if head motion exceeded 3 mm of translation or 3° of rotation, or if scan coverage was inadequate.[23–25] As a result, 3 participants in the drug group were excluded, yielding 12 valid datasets; in the acupuncture group, 4 participants were excluded, yielding 11 valid datasets. Although 10 healthy controls were initially planned, only 7 were successfully recruited; after excluding 1 participant for excessive head motion, 6 valid control datasets remained for analysis (Figure 1).

Inclusion and Exclusion Criteria

Inclusion criteria were as follows: 1) participants of any gender, right-handed, aged 50–90 years; 2) patients in the medication or acupuncture group met the diagnostic criteria outlined in the 2018 Chinese Guidelines for the Diagnosis and Treatment of Dementia and Cognitive Impairment (II): Guidelines for the Diagnosis and Treatment of AD;[26] 3) no acupuncture treatment within the previous six months; 4) the patient or their legal guardian voluntarily agreed to participate and provided written informed consent.

Exclusion criteria were as follows: 1) Patients with severe organic diseases of the heart, liver, or kidneys confirmed by imaging examinations such as ultrasound, CT, or MRI (eg., liver cirrhosis, renal failure, heart failure, etc).; patients with mental disorders including depression, anxiety disorder, schizophrenia, etc., definitely diagnosed by psychiatrists; 2) Patients with neurological disorders that may affect brain function and cognitive function were excluded, such as Parkinson's disease, cerebral infarction, cerebral hemorrhage, epilepsy, intracranial space-occupying lesions, and severe traumatic brain injury.3) severe visual or hearing impairment that interfered with completion of the assessments; 4) intolerance to donepezil hydrochloride or acupuncture treatment; 5) Patients who had received medications affecting cerebral metabolism, cerebral blood flow, and central nervous system function within the past 1 month were excluded. 6) participation in other clinical trials concurrently; 7) contraindications to MRI examination.

Treatment Regimen

Drug Group

Participants in the drug group received oral donepezil hydrochloride tablets (Eisai China Inc.; approval No. H20050978; 5 mg/tablet). The medication was administered once daily at a dose of 5 mg before bedtime. After 4 consecutive weeks, the dose was increased to 10 mg, with a total treatment duration of 6 weeks.

Acupuncture Group

On the basis of the same pharmacological treatment used in the drug group, participants in the acupuncture group received acupuncture according to the "Yizhi Tiaoshen" prescription (Figure 2). The selected acupoints were Baihui (GV20), Sishencong (EX-HN1), Shenmen (HT7), Neiguan (PC6), Zusanli (ST36), Sanyinjiao (SP6), and Xuanzhong (GB39), with localization based on the national standard Nomenclature and Location of Acupuncture Points (GB/T 12346–2006).[27]

Disposable sterile filiform needles (Huacheng brand; 0.30×25 mm or 0.30×40 mm; Beijing Medical Device Registration No. 20182271110) were used. The needling depths were as follows: Baihui, transverse insertion 13–20 mm; Sishencong, transverse insertion toward Baihui 13–20 mm; Shenmen, perpendicular insertion 8–13 mm; Neiguan, perpendicular insertion 13–24 mm; Zusanli and Sanyinjiao, perpendicular insertion 25–38 mm; and Xuanzhong, perpendicular insertion 13–20 mm. After achieving deqi (arrival of qi), the first four acupoints were manipulated with a mild reinforcing–reducing technique, while the remaining three acupoints were stimulated using lifting and thrusting and rotating reinforcement for approximately 1 minute. Needles were retained for 30 minutes, with additional manipulation performed once at the 15-minute mark. Treatments were administered once daily, six times per week, for a total of 6 weeks.

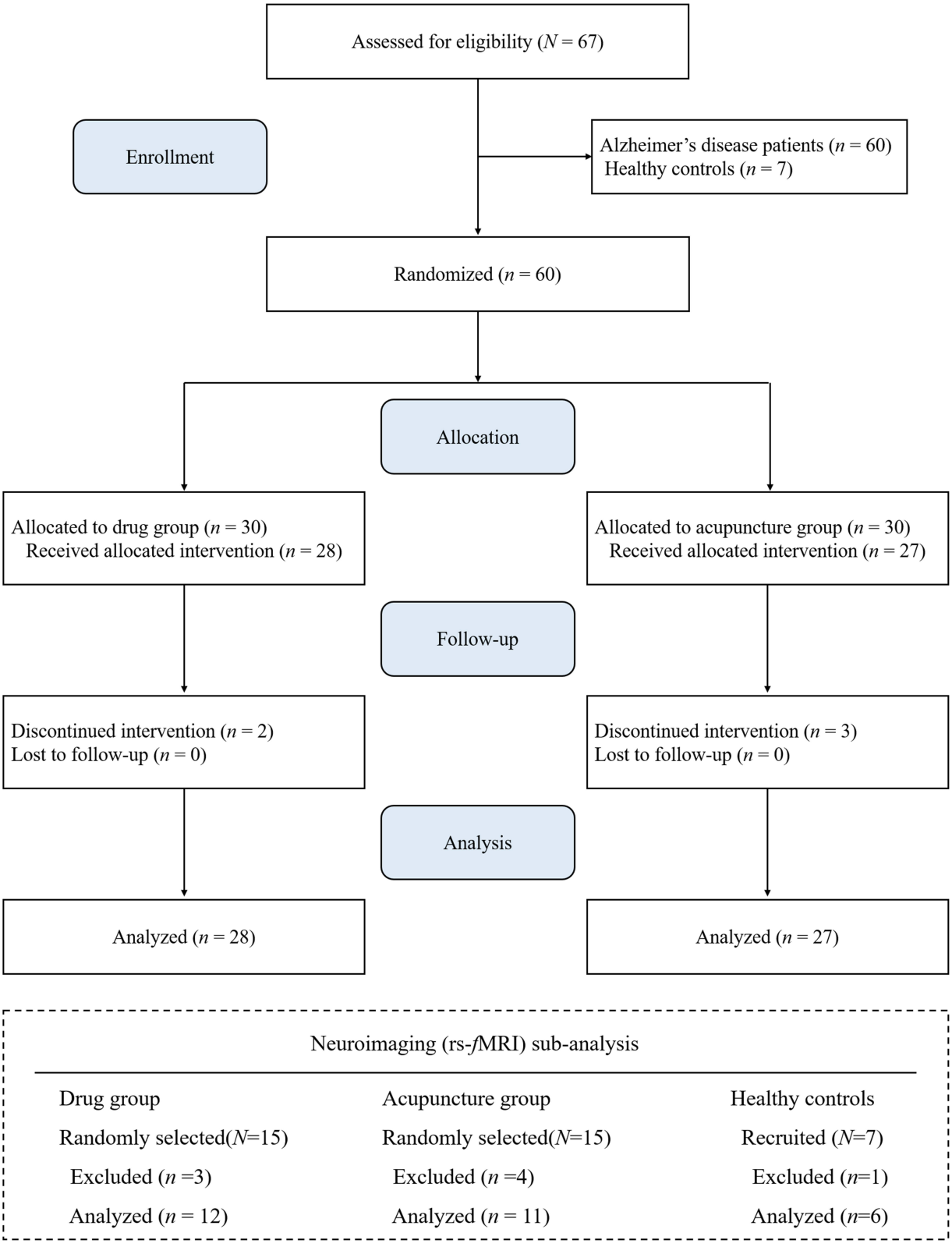

Figure 1 Flowchart of the trial.

Note: A total of 67 participants were assessed for eligibility, including 60 patients with Alzheimer's disease (AD) and 7 healthy controls (HC). AD patients were randomized into the Drug group (η=30) and the Acupuncture group (η=30). For clinical efficacy, 28 patients in the Drug group and 27 in the Acupuncture group were included in the final analysis.For the resting-state fMRI (rs-fMRI) study, 15 patients from each group and 7 healthy controls were enrolled for scanning. After excluding data due to quality control, the final neuroimaging analyses included 12 patients in the Drug group, 11 in the Acupuncture group, and 6 HCs.

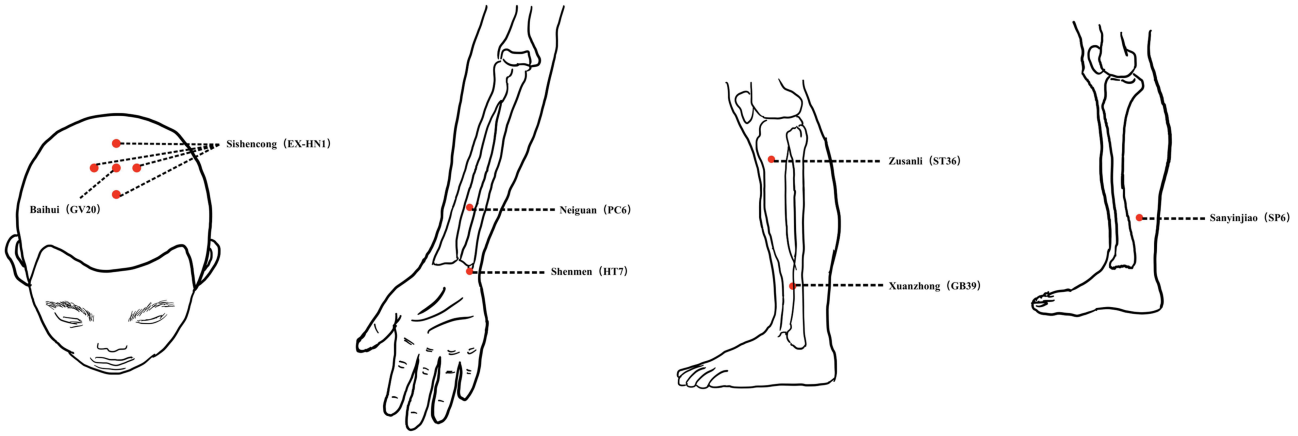

Figure 2 Acupoints for the acupuncture group.
Note: The schematic illustrates the specific acupoints selected for the " Yizhi Tiaoshen" prescription. The locations include Baihui (GV20) and Sishencong (EX-HN1) on the head; Neiguan (PC6) and Shenmen (HT7) on the upper limb; and Zusanli (ST36), Xuanzhong (GB39), and Sanyinjiao (SP6) on the lower limb.

Clinical Evaluation Scale

Both groups underwent the following assessments before and after treatment. All scales and neuropsychological evaluations were administered by a qualified neuropsychologist who was blinded to group allocation.

Montreal Cognitive Assessment–Basic, Chinese Version (MoCA-B)

The MoCA-B consists of 10 subdomains assessing executive function, verbal fluency, orientation, calculation, abstraction, delayed recall, visuoperceptual ability, naming, and attention. The total score is 30 points. Based on years of education, the cutoff values for cognitive impairment are ≤19 for individuals with ≤6 years of education, ≤22 for those with 7–12 years of education, and ≤24 for those with more than 12 years of education. Lower scores reflect more severe cognitive dysfunction.[28]

Rs-fMRI Scanning Protocol

Healthy controls underwent a single rs-*f*MRI scan, whereas patients in both groups received rs-*f*MRI scans before and after treatment. All imaging was performed using a 3.0-T MRI scanner (Ingenia Elition X, Philips Healthcare, The Netherlands) equipped with a 32-channel phased-array head coil and high-attenuation noise-reduction earplugs. Upon entering the scanner room, participants were positioned supine with their heads secured using a fitted head holder to minimize voluntary and involuntary movements. Earplugs were provided to reduce external noise interference. Participants were instructed to remain awake, keep their eyes closed, breathe steadily, and avoid engaging in any deliberate cognitive activity during the scan. The scanning procedure included a 2-min 38-s high-resolution three-dimensional T1-weighted structural scan followed by an 8-min 6-s resting-state *f*MRI acquisition. After confirming the absence of gross abnormalities such as hemorrhage or tumors on routine imaging, structural images were acquired using a fast field echo (FFE) gradient-echo sequence with the following parameters: repetition time (TR) = 6.6 ms; echo time (TE) = 3 ms; flip angle = 8°; voxel size = 1 mm × 1 mm × 1 mm; field of view (FOV) = 240 mm × 240 mm; slice thickness = 1 mm; no interslice gap; 170 slices in total. Resting-state functional images were acquired using an axial echo-planar imaging (EPI) sequence with the following parameters: TR = 2000 ms; TE = 30 ms; flip angle = 90°; voxel size = 2 mm × 2 mm × 2 mm; FOV = 224 mm × 224 mm; slice thickness = 2 mm; 42 slices; and 240 whole-brain volumes collected.

Data Processing of Rs-fMRI

Rs-*f*MRI data were preprocessed and analyzed using the RESTplus V1.27 toolbox running on Statistical Parametric Mapping (SPM12) within the MATLAB 2017b environment. The preprocessing steps included the following: (1) Format conversion and discarding initial volumes: Raw data were converted from DICOM to NIFTI format using MRIcronGL. The first 10 time points were removed to eliminate signal instability and to minimize fluctuations caused by participant adaptation at the

beginning of the scan. (2) Slice-timing correction: In this study, rs-*f*MRI data were acquired from the vertex to the base of the skull using an interleaved odd–even scanning order ([41:-2:1; 42:-2:2]). Slice-timing correction was applied to compensate for temporal differences in slice acquisition. (3) Head-motion correction: Participants with head movement exceeding 3.0 mm of translation or 3.0° of rotation were excluded. (4) Spatial normalization: The new_segment algorithm was used to first coregister T1-weighted structural images to the rs-*f*MRI images. T1 images were then segmented into gray matter, white matter, cerebrospinal fluid, skull, soft tissue, and meninges. The segmented images were resampled to 3 mm × 3 mm × 3 mm voxels and normalized to the Montreal Neurological Institute (MNI) standard space. (5) Spatial smoothing: A Gaussian kernel with 6 mm full width at half maximum (FWHM) was applied to the normalized images to improve the signal-to-noise ratio. (6) Nuisance regression: Friston-24 head-motion parameters, cerebrospinal fluid signals, and white matter signals were regressed out to reduce physiological and movement-related confounds. (7) Detrending: Linear detrending was performed to remove slow signal drifts caused by scanner heating or temporal instability. (8) Temporal filtering: A band-pass filter (0.01–0.08 Hz) was applied to reduce high-frequency physiological noise and low-frequency drifts, retaining the frequency range relevant for spontaneous neural activity.

ICA was performed following the steps below: (1) Data preprocessing: Preprocessing was conducted using the Variational Control Group Normalization method. (2) Estimation and decomposition of independent components: The Infomax algorithm was applied to decompose the data into independent components. A total of 32 components were automatically estimated in this study. (3) Principal component analysis (PCA): Standard PCA was used at the individual level, while the Subject-Specific algorithm was applied at the group level to extract principal components. (4) Stability assessment: The ICASSO algorithm was employed to evaluate the stability and reliability of the ICA decomposition. (5) Back-reconstruction: The Spatial–Temporal Regression algorithm was used to back-reconstruct individual-level component maps from the group ICA results. (6)*Z*-score transformation: The reconstructed component maps were converted into Z-score maps to approximate a normal distribution and facilitate statistical comparison. (7) Component identification: Components with Z-scores ≥ 1 were extracted and subjected to spatial correlation analysis with the Power264 functional atlas. The component showing the highest spatial similarity was identified and used to determine the constituent brain regions of the FPN.

GCA computation was conducted as follows: All clusters within the identified brain network were defined as regions of interest (ROIs). For each ROI, a spherical region with a radius of 6 mm was constructed around its central coordinate. The time series of all voxels within each sphere were extracted and averaged to obtain a representative time series for that ROI. Bivariate coefficient GCA was then performed for all ROIs. Each ROI was analyzed in two directions: the causal influence exerted by the ROI on other regions ($x \rightarrow y$) and the causal influence imposed by other regions on the ROI ($y \rightarrow x$). Pearson correlation coefficients between the mean time series of each pair of ROIs were calculated to generate GCA values, which served as indicators of effective connectivity for subsequent statistical analyses.

GCA node degree computation was conducted as follows: To evaluate the centrality of nodes within the network, out-degree, in-degree, and total degree were calculated for each ROI. Out-degree represented the number of directional connections projecting from the node to other nodes, while in-degree represented the number of connections projecting into the node. Total degree was defined as the sum of out-degree and in-degree. Nodes with high in-degree were considered central targets within the network, whereas nodes with high out-degree were regarded as central sources. A node was classified as a core region of the network if its total degree exceeded the mean total degree of all nodes plus one standard deviation.

Statistical Analysis

Clinical Data Analysis

All clinical data were analyzed using SPSS version 26.0. Measurement data were expressed as mean ± standard deviation ($\bar{\chi} \pm s$). For within-group comparisons, paired t-tests were used when variances were homogeneous, and the Wilcoxon signed-rank test was applied when variances were heterogeneous. For between-group comparisons, independent-samples t-tests were used when variances were homogeneous, and the t′-test was applied when variances were unequal. Two-tailed tests were applied throughout, with $P < 0.05$ considered statistically significant.

Rs-fMRI Data Analysis

Paired t-tests were used to examine within-group differences in GCA values before and after treatment in both the drug and acupuncture groups. Two-sample t-tests were employed to compare GCA values between AD patients and healthy controls at pre-treatment, as well as between the drug and acupuncture groups after treatment. A voxel-level threshold of $P < 0.05$ (uncorrected) was considered statistically significant. Due to the relatively small sample size and the exploratory nature of this study, multiple comparison correction was not performed for the fMRI indicators.

Results

Demographic Characteristics and Cognitive Scale Scores

A total of 55 patients with AD were included in the final analysis, comprising 28 participants in the drug group and 27 in the acupuncture group. Prior to treatment, no significant differences were observed between the two groups in age, gender, disease duration, educational level, and MoCA-B scores ($P > 0.05$; Table 1).

After treatment, both groups exhibited significant improvements in cognitive performance. In the drug group, MoCA-B scores increased from 13.30 ± 3.14 to 15.71 ± 3.72. Likewise, the acupuncture group demonstrated marked cognitive enhancement, with MoCA-B scores rising from 13.50 ± 2.86 to 16.81 ± 3.89. Notably, post-treatment MoCA-B scores in the acupuncture group were significantly higher than those in the drug group ($P < 0.05$; Table 2), suggesting that acupuncture provided a superior improvement in global cognitive function. Furthermore, relative to baseline, the mean change in MoCA-B scores after treatment was greater than 2 points in both the drug group and the acupuncture group. Comparison between the two groups revealed a statistically significant difference in the magnitude of change ($P < 0.05$; Table 3).

Table 1 Demographic and Cognitive Characteristics of the Study Participants

Item	Drug Group (n=28)	Acupuncture Group (n=27)	Statistical	*P* value
Gender (M/F)	10/18	8/19	χ^2=0.23	0.63
Age (years)	69.21±8.275	71.37±7.697	t=−1.00	0.32
Disease duration (months)	22.21±12.59	25.04±10.65	t=−0.90	0.37
Education level (years)	8.73±3.64	8.52±3.65	t=0.22	0.83
MoCA-B scores	13.30±3.14	13.50±2.86	t=0.25	0.80

Table 2 Comparison of Cognitive Scores Between the Two Groups at Pre- and Post-Treatment

Groups	MoCA-B Scores		Statistical	*P* value
	Pre-Treatment	Post-Treatment		
Drug group (n=28)	13.30±3.14	15.71±3.72	t=−9.11	<0.001
Acupuncture group (n=27)	13.50±2.86	16.81±3.89	t=−17.39	<0.001
Statistical	t=0.25	t=−2.04		
P value	0.80	0.046		

Table 3 Comparison of Changes in MoCA-B Scores Before and After Treatment Between the Two Groups

Groups	MoCA-B Scores	Statistical	*P* value
Drug group (n=28)	2.21±1.29	t=−6.63	<0.001
Acupuncture group (n=27)	4.29±1.03		

https://doi.org/10.2147/NDT.S601136

Neuroimaging results

Demographic Data

This analysis included 23 patients with AD (12 in the drug group and 11 in the acupuncture group) and 6 age-, gender-, and education-matched healthy controls. Compared with pre-treatment, no significant differences were observed between the two AD groups in age, gender, disease duration, educational level, and MoCA-B scores ($P > 0.05$; Table 4).

The ICA Analysis results

In this study, ICA of the *f*MRI data from all participants identified the FPN as comprising 14 voxel clusters. The main brain regions included the left cerebellum Crus II; right cerebellum Crus I; right inferior frontal gyrus, orbital part; middle temporal gyrus; middle frontal gyrus; right insula; inferior parietal lobule; left median cingulate and paracingulate gyri; left superior frontal gyrus, medial and the precuneus. The detailed composition of the FPN is presented in Table 5 and illustrated in Figure 3.

Intra-Group and Inter-Group Comparison of GCA Within the FPN

(1) Differences in effective connectivity within the FPN between AD group and HC group

Compared with the HC group, patients with AD exhibited a predominant pattern of reduced effective connectivity among ROIs within the FPN, mainly involving parietal and temporal regions. Specifically, significantly decreased GCA values ($P < 0.05$) were observed in the effective connectivity from the left middle temporal gyrus to the right inferior parietal lobule and the left median cingulate and paracingulate gyri; from the left inferior parietal lobule to the right inferior temporal gyrus and right inferior parietal lobule; from the left medial frontal gyrus, orbital part to the left cerebellum Crus II; from the right inferior parietal lobule to the right cerebellum Crus I; and from the left precuneus to the right insula. In contrast, enhanced effective connectivity was observed in several frontal and temporal regions, including increased GCA values ($P < 0.05$) from the right inferior frontal gyrus, orbital part and right inferior temporal

Table 4 Demographic and Cognitive Characteristics of Study Participants in Neuroimaging Analysis

Item	Drug Group (n=12)	Acupuncture Group (n=11)	Statistical	*P* value
Gender (M/F)	3/9	3/8	χ^2=0.15	1
Age (years)	68.33±6.67	69.45±9.40	*t*=−0.33	0.74
Disease duration (months)	19.42±9.62	28.55±13.20	*t*=−1.91	0.07
Education level (years)	7.96±3.68	10.64±3.17	*t*=−1.86	0.07
MoCA-B scores	14.00±2.83	13.37±3.93	t=0.19	0.85

Table 5 Components of the FPN

Cluster	Brain Regions	AAL	MNI Coordinates			Voxel
			X	Y	Z	
Cluster 1	L_Cerebelum_Crus II	93	−39	−72	−39	24
	L_Cerebelum_Crus I	91				26
Cluster 2	R_Cerebelum_Crus I	92	9	−81	−27	125
	L_Cerebelum_Crus I	91				15
	Cerebelum_Crus II	93, 94				82
	R_Cerebelum_6	100				26
	Vermis_7	113				3
	R_Cerebelum_7b	102				1
Cluster 3	R_ORBinf	16	15	6	−24	6
	R_ORBsup	6				4
	R_PHG	40				2

(*Continued*)

Table 5 (Continued).

Cluster	Brain Regions	AAL	MNI Coordinates			Voxel
			X	Y	Z	
Cluster 4	L_MTG	85	−63	−39	−9	195
	L_ITG	89				93
Cluster 5	R_MTG	86	60	−45	−12	143
	R_ITG	90				46
Cluster 6	L_MFG	7	−42	51	−3	670
	L_IFGtriang	13				530
	L_PreCG	1				267
	L_IFGoperc	11				195
	L_ORBinf	15				184
	L_SFGdor	3				121
	L_ORBmid	9				75
	L_INS	29				60
	L_ORBsup	5				27
	L_PoCG	57				22
	L_TPOsup	83				19
	L_ROL	17				13
	L_SFGmed	23				10
	L_HES	79				8
	L_STG	81				6
Cluster 7	R_MFG	8	33	63	3	618
	R_IFGtriang	14				252
	R_IFGoperc	12				159
	R_ORBinf	16				153
	R_SFGdor	4				132
	R_ORBmid	10				91
	R_INS	30				82
	R_ORBsup	6				31
	R_TPOsup	84				27
	R_PreCG.	2				15
	R_ROL	18				7
	R_SFGmed	24				1
Cluster 8	R_INS	30	42	−9	−9	9
	R_STG	82				11
Cluster 9	L_IPL	61	−39	−63	54	508
	L_ANG	65				190
	L_SPG	59				142
	L_MOG	51				51
	L_PoCG	57				17
	L_SOG	49				3
	L_PCUN	67				2
	L_SMG	63				1
Cluster 10	R_IPL	62	42	−57	57	240
	R_ANG	66				178
	R_SMG	64				136
	R_SPG.	60				97
	R_PoCG	58				8
	R_SOG	50				8

(*Continued*)

Table 5 (Continued).

Cluster	Brain Regions	AAL	MNI Coordinates			Voxel
			X	Y	Z	
Cluster 11	L_DCG	33	0	−33	36	35
	R_DCG	34				22
	R_PCUN	68				2
Cluster 12	L_SFGmed	23	3	27	45	71
	R_SFGmed	24				8
	SMA	19, 20				77
Cluster 13	R_PCUN	68	9	−72	48	50
	R_SPG	60				2
Cluster 14	L_PCUN	67	−6	−72	48	19
	L_SPG	59				1

Notes: A cluster refers to a relatively large voxel cluster containing multiple brain regions. Brain regions shown in bold represent the primary regions corresponding to the peak voxel within each cluster, whereas the remaining regions are considered subsidiary regions. AAL denotes the Automated Anatomical Labeling atlas. The peak voxel indicates the location with the most significant effect. MNI refers to the Montreal Neurological Institute coordinate system. The same notation applies to the following tables.

Abbreviations: L, left; R, right; ORBinf, Inferior frontal gyrus, orbital part; ORBsup, Frontal_Sup_Orb, Superior frontal gyrus, orbital part; PHG, Parahippocampal gyrus; MTG, Middle temporal gyrus; ITG, Inferior temporal gyrus; MFG, Middle frontal gyrus; FGtriang, Inferior frontal gyrus, triangular part; PreCG, Precentral gyrus; IFGoperc, Inferior frontal gyrus, opercular part; SFGdor, Superior frontal gyrus, dorsolateral; ORBmid, Medial frontal gyrus, orbital part; INS, Insula; PoCG, Postcentral gyrus; TPOsup, Temporal pole (superior temporal gyrus); ROL, Rolandic operculum; SFGmed, Superior frontal gyrus, medial; HES, Heschl gyrus; STG, Superior temporal gyrus; IPL, Inferior parietal lobule (including supramarginal and angular gyri); ANG, Angular gyrus; SPG, Superior parietal gyrus; MOG, Middle occipital gyrus; SOG, Superior occipital gyrus; PCUN, Precuneus; SMG, Supramarginal gyrus; DCG, Median cingulate and paracingulate gyri; SMA, Supplementary motor area.

gyrus to the right superior frontal gyrus, medial; from the right inferior parietal lobule to the left middle temporal gyrus and left medial frontal gyrus, orbital part; and from the left median cingulate and paracingulate gyri to the left middle temporal gyrus (Table 6, Figure 4).

Relative to HC group, the mean node degree of effective connectivity within the FPN in AD group was 1.92 ± 1.31. The right inferior parietal lobule (total degree = 5) and the left middle temporal gyrus (total degree = 4) were identified as core regions of the FPN. Among them, the right inferior parietal lobule functioned as a central source node, while the right superior frontal gyrus, medial; left middle temporal gyrus and right inferior parietal lobule served as central target nodes within the FPN (Figure 5).

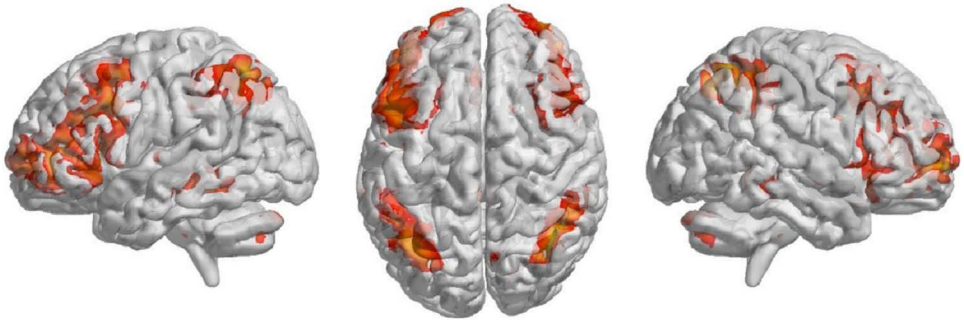

Figure 3 Three-dimensional representation of the constituent brain regions of the FPN.
Note: The spatial map of the FPN was extracted using group-level independent component analysis (ICA) from resting-state fMRI data. The highlighted orange-red regions indicate the key regions of the network.

Table 6 ROI1→ROI2 Connections Within the FPN Showing Significant Differences in GCA Values Between the AD and HC Groups

ROI1			ROI2			T value	*P* value
Brain Regions	**MNI**	**Voxel**	**Brain Regions**	**MNI**	**Voxel**		
AD group>HC group							
R_ORBinf	15,6,-24	28	R_SFGmed	3,27,45	156	2.445	0.021
R_ITG	60,-45,-12	189	R_SFGmed	3,27,45	156	2.105	0.045
R_IPL	42,-57,57	669	L_MTG	−63,-39,-9	288	2.678	0.012
L_DCG	0,-33,36	59	L_MTG	−63,-39,-9	288	2.596	0.015
R_IPL	42,-57,57	669	L_ORBmid	−42,51,-3	2266	3.071	0.005
AD group<HC group							
L_MTG	−63,-39,-9	288	R_IPL	42,-57,57	669	−2.102	0.045
L_MTG	−63,-39,-9	288	L_DCG	0,-33,36	59	−2.064	0.049
L_IPL	−39,-63,54	936	R_IPL	42,-57,57	669	−2.344	0.027
L_ORBmid	−42,51,-3	2266	L_Cerebelum_Crus II	−39,-72,-39	50	−2.230	0.034
R_IPL	42,-57,57	669	R_Cerebelum_Crus I	9, −81,-27	252	−2.700	0.012
L_IPL	−39,-63,54	936	R_ITG	60,-45,-12	189	−2.152	0.041
L_PCUN	−6,-72,48	20	R_INS	42,-9,-9	22	−3.026	0.005

(2) Within-group differences in effective connectivity within the FPN at pre- and post-treatment in the drug group

Compared with pre-treatment, abnormal effective connectivity among FPN-related brain regions in patients with AD showed partial normalization after treatment. Specifically, enhanced effective connectivity was observed among frontal regions and between the cerebellum and parietal cortex, including significantly increased GCA values from the left

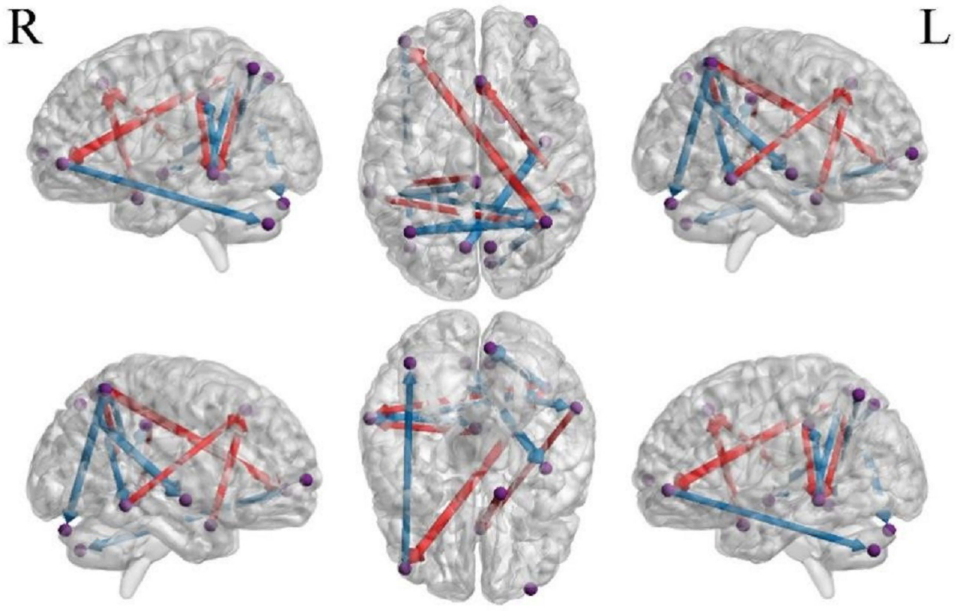

Figure 4 Effective connectivity between ROIs within the FPN showing significant differences in GCA values between the AD and the HC groups.
Note: Purple spheres represent the regions of interest (ROIs) within the FPN. Arrows denote the directionality of Granger causal influences, indicating significant causal relationships between brain regions (P<0.05). Red lines represent enhanced effective connectivity, while blue lines indicate reduced effective connectivity. The thickness of the lines reflects the magnitude of the increase or decrease in connectivity strength.Compared with HCs, AD patients exhibited decreased effective connectivity among FPN ROIs, including: L_MTG→R_IPL,L_MTG→L_DCG,L_IPL→R_IPL,L_ORBmid→L_Cerebelum_Crus II,R_IPL→R_Cerebelum_Crus I,L_IPL→R_ITG,L_PCUN→R_INS (P<0.05). Compared with HCs, the ROIs showing increased effective connectivity within the FPN in AD patients included:R_ORBinf→R_SFGmed,R_ITG→R_SFGmed, R_IPL→L_MTG,L_DCG→L_MTG,R_IPL→L_ORBmid(P<0.05).

https://doi.org/10.2147/NDT.S601136

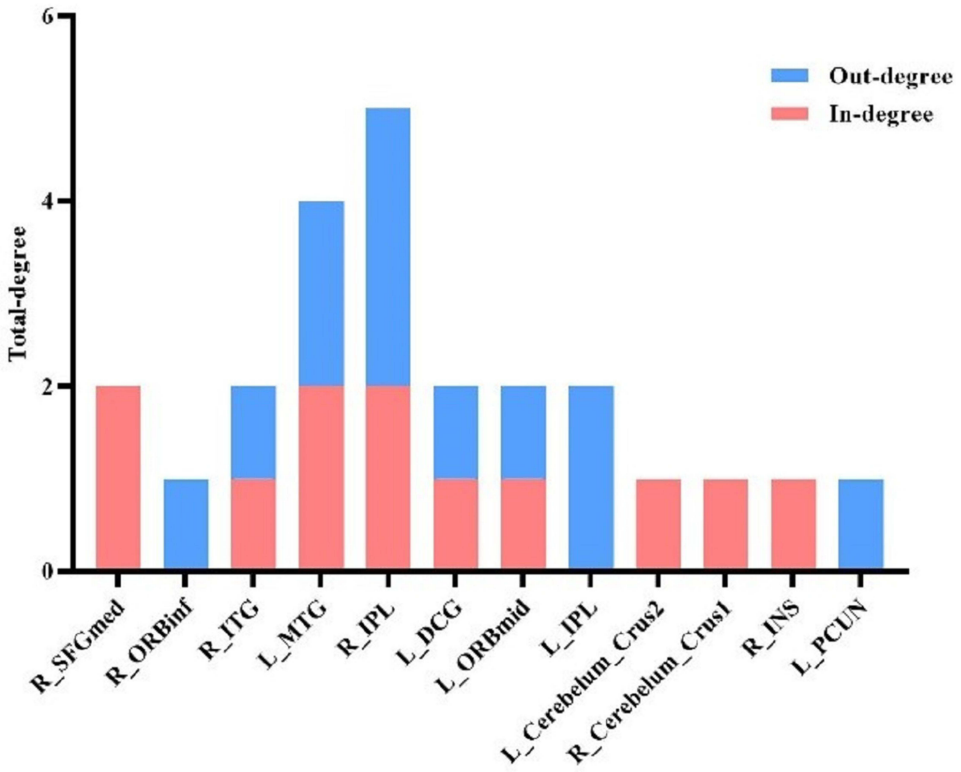

Figure 5 Comparison of total node degree of effective connectivity within the FPN between the AD and the HC groups.
Note: The bar graph illustrates the nodal characteristics of the (FPN) in patients with AD compared with HCs. The y-axis represents the degree count. where blue bars indicate Out-degree (efferent connections) and red bars indicate In-degree (afferent connections). The R_IPL and L_MTG were identified as core regions within the FPN. Specifically, The R_IPL served as both a central source node and a central target node. Additionally, the R_SFGmed and L_MTG functioned primarily as central target nodes.

median cingulate and paracingulate gyri to the right medial superior frontal gyrus, and from the left cerebellum Crus II to the right precuneus ($P < 0.05$). In contrast, reduced frontoparietal effective connectivity was observed, characterized by a significant decrease in GCA values from the right inferior parietal lobule to the left medial frontal gyrus, orbital part ($P < 0.05$) (Table 7, Figure 6).

Compared with pre-treatment, the mean node degree of effective connectivity within the FPN after treatment was 1, with no core regions, central target nodes, or central source nodes identified. The left cerebellum Crus II, left median cingulate and paracingulate gyri, and right inferior parietal lobule primarily served as information output nodes within the network, whereas the right precuneus; right superior frontal gyrus, medial; and left medial frontal gyrus, orbital part mainly functioned as information input nodes (Figure 7).

Table 7 ROI1→ROI2 Connections Within the FPN Showing Significant Differences in GCA Values at Pre- and Post-Treatment in the Drug Group

ROI1			**ROI2**			**T value**	***P* value**	
Brain Regions	**MNI**	**Voxel**	**Brain Regions**	**MNI**	**Voxel**			**Cohen's d**
Post-treatment>Pre-treatment								
L_Cerebelum_Crus II L_DCG	-39,-72,-39 0,-33,36	50 59	R_PCUN R_SFGmed	9,-72,48 3,27,45	28 169	2.574 2.654	0.026 0.022	0.74 0.77
Post-treatment<Pre-treatment								
R_IPL	42,-57,57	669	L_ORBmid	-42,51,-3	2266	-2.330	0.040	0.67

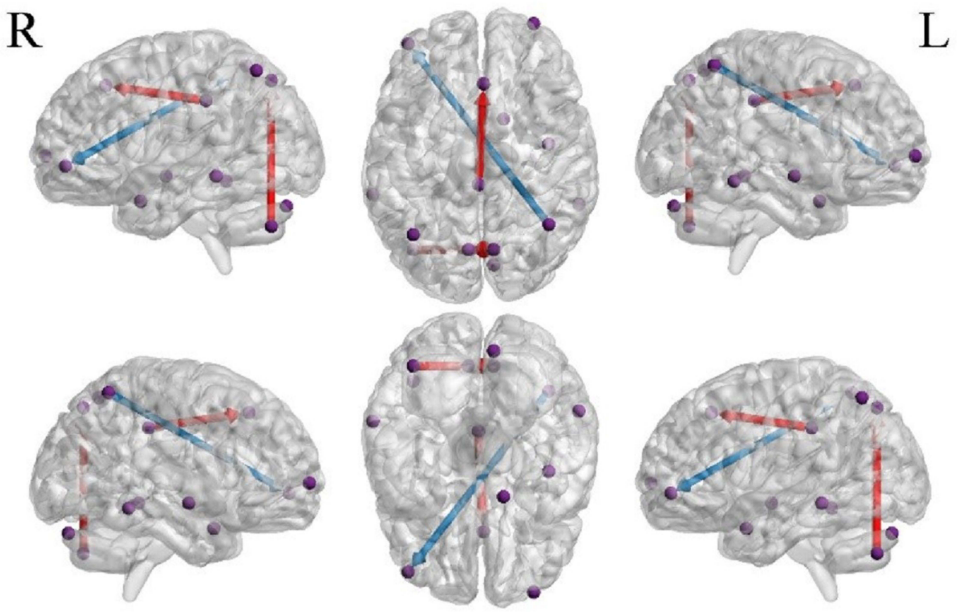

Figure 6 Effective connectivity between ROIs within the FPN showing significant differences in GCA values at pre- and post-treatment in the drug group.
Note: Purple spheres represent the regions of interest (ROIs) within the FPN. Arrows denote the directionality of Granger causal influences, indicating significant causal relationships between brain regions (P<0.05). Red lines represent enhanced effective connectivity, while blue lines indicate reduced effective connectivity. The thickness of the lines reflects the magnitude of the increase or decrease in connectivity strength. Changes in effective connectivity within the FPN in the drug group following treatment. Compared with baseline, regions showing increased effective connectivity in AD patients included the L_Cerebelum_Crus II→R_PCUN, L_DCG→R_SFGmed (P<0.05). compared with baseline, regions showing decreased effective connectivity included the R_IPL→L_ORBmid (P<0.05).

(3) Within-group differences in effective connectivity within the FPN at pre- and post-treatment in the acupuncture group

Compared with pre-treatment, patients with AD in the acupuncture group exhibited significant changes in effective connectivity within the frontoparietal network after treatment. Specifically, GCA values from the left precuneus to the right precuneus were significantly increased ($P < 0.05$), whereas GCA values from the right inferior parietal lobule to the left middle temporal gyrus and from the right superior frontal gyrus, medial to the right superior frontal gyrus, dorsolateral were significantly decreased ($P < 0.05$) (Table 8, Figure 8).

Compared with pre-treatment, the mean node degree of effective connectivity within the FPN after treatment was 1, with no core regions, central target nodes, or central source nodes identified. The left precuneus, right inferior parietal lobule, and right superior frontal gyrus, medial primarily functioned as information output nodes, whereas the right precuneus, left middle temporal gyrus, and right superior frontal gyrus, dorsolateral served as information input nodes within the network (Figure 9).

(4) Between-group differences in effective connectivity within the FPN after treatment

After treatment, between-group comparisons revealed significant differences in effective connectivity within the FPN between the drug group and the acupuncture group. In the acupuncture group, patients with AD exhibited significantly higher GCA values than those in the drug group in effective connectivity from the right insula and right medial superior frontal gyrus to the right cerebellum Crus I, as well as from the right insula and left precuneus to the left middle temporal gyrus ($P < 0.05$). In contrast, patients in the drug group showed significantly higher GCA values than those in the acupuncture group in effective connectivity from the left cerebellum Crus II to the right superior frontal gyrus, medial; from the right cerebellum Crus I to the right insula; from the left middle temporal gyrus and right inferior temporal gyrus to the right superior frontal gyrus, dorsolateral; and from the right superior frontal gyrus, dorsolateral to the left cerebellum Crus II ($P < 0.05$) (Table 9, Figure 10).

Compared between groups, the mean node degree of effective connectivity within the FPN in AD patients after acupuncture intervention was 2.25 ± 0.89, with no core regions identified. The right insula functioned as the central source node, whereas the right cerebellum Crus I, left middle temporal gyrus, and right superior frontal gyrus, dorsolateral served as central target nodes within the network (Figure 11).

https://doi.org/10.2147/NDT.S601136

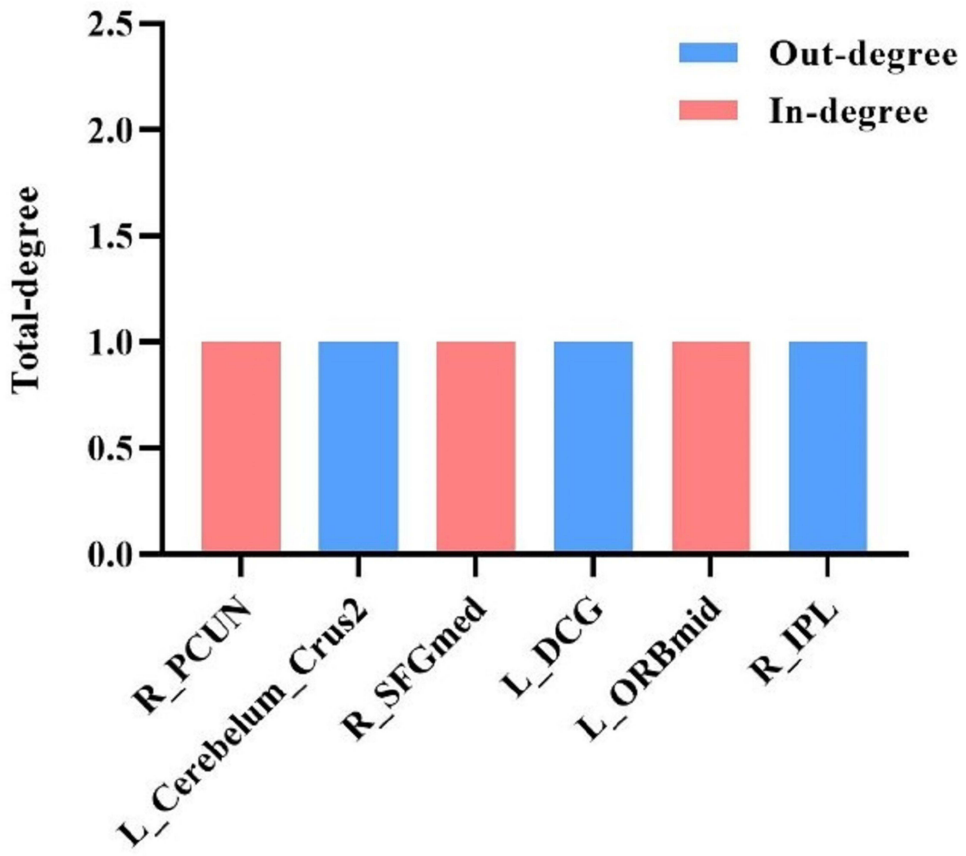

Figure 7 Comparison of total node degree of effective connectivity within the FPN at pre- and post-treatment in the drug group.
Note: The bar graph illustrates the nodal characteristics of the FPN following the drug group treatment. The y-axis represents the degree count. where blue bars indicate Out-degree (efferent connections) and red bars indicate In-degree (afferent connections). No specific core regions (hubs) were identified in the drug group after treatment. The L_Cerebelum_Crus2, L_DCG and R_IPL function as information output nodes. Conversely, the R_PCUN, R_SFGmed and L_ORBmid serve as information input nodes.

Discussion

The results of the present study demonstrate that the "Yizhi Tiaoshen" acupuncture regimen combined with donepezil hydrochloride significantly improves the learning effect in patients with Alzheimer's disease, and the therapeutic efficacy is superior to that of donepezil hydrochloride monotherapy. These findings are consistent with previous studies[29] and provide preliminary evidence for the clinical effectiveness of the "Yizhi Tiaoshen" acupuncture regimen in the treatment of Alzheimer's disease. However, further verification is needed in studies with larger sample sizes and longer follow-up durations.

Table 8 ROI1→ROI2 Connections Within the FPN Showing Significant Differences in GCA Values at Pre- and Post-Treatment in the Drug Group

ROI1			**ROI2**			**T value**	***P* value**	
Brain Regions	**MNI**	**Voxel**	**Brain Regions**	**MNI**	**Voxel**			**Cohen's d**
Post-treatment>Pre-treatment								
L_PCUN	−6,-72,48	20	R_PCUN	9,-72,48	52	2.494	0.032	0.75
Post-treatment<Pre-treatment								
R_IPL	42,-57,57	669	L_MTG	−63,-39,-9	288	−2.340	0.041	0.71
R_SFGmed	3,27,45	156	R_SFGdor	33,63,3	1622	−2.927	0.015	0.88

 https://doi.org/10.2147/NDT.S601136

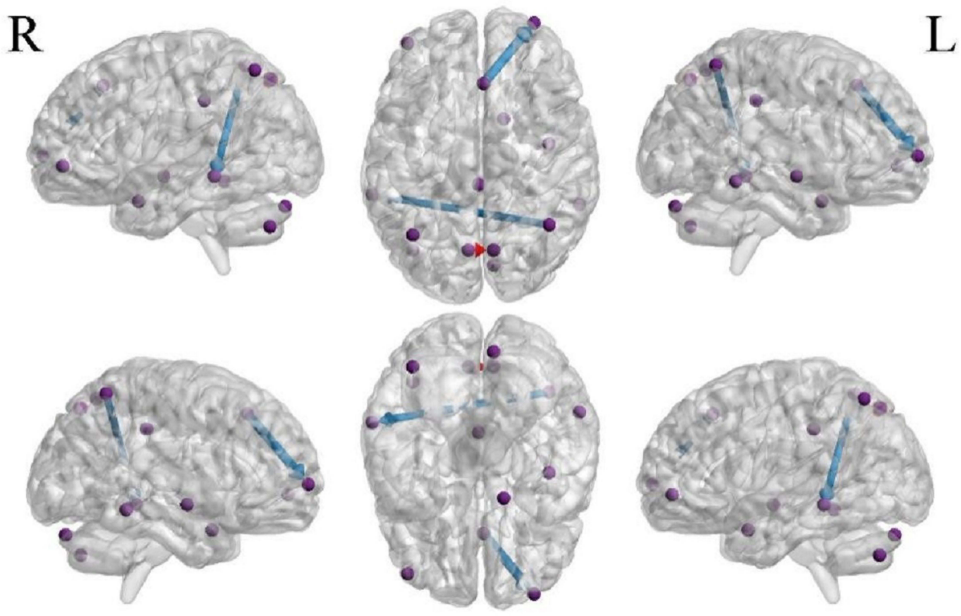

Figure 8 Effective connectivity between ROIs within the FPN showing significant differences in GCA values at pre- and post-treatment in the acupuncture group.
Note: Purple spheres represent the regions of interest (ROIs) within the FPN. Arrows denote the directionality of Granger causal influences, indicating significant causal relationships between brain regions (P<0.05). Red lines represent enhanced effective connectivity, while blue lines indicate reduced effective connectivity. The thickness of the lines reflects the magnitude of the increase or decrease in connectivity strength. Changes in effective connectivity within the FPN in the acupuncture group following treatment.Compared with baseline, regions showing increased effective connectivity in AD patients included the L_PCUN→R_PCUN(P<0.05).compared with baseline, regions showing decreased effective connectivity included the R_IPL→L_MTG, R_SFGmed→R_SFGdor(P<0.05).

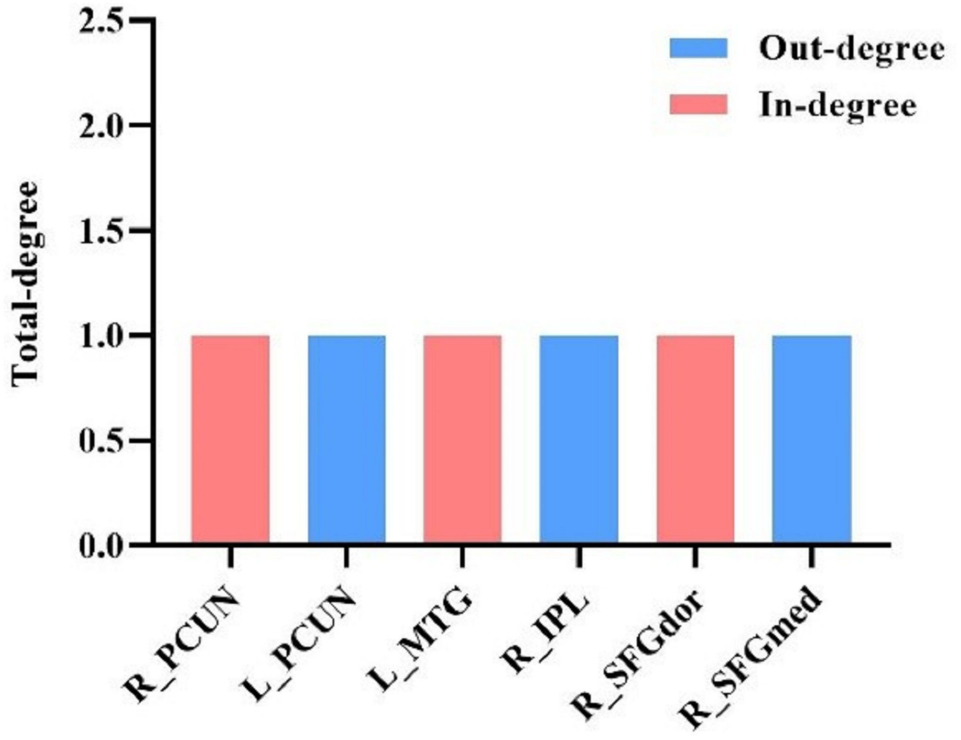

Figure 9 Comparison of total node degree of effective connectivity within the FPN at pre- and post-treatment in the acupuncture group.
Note: The bar graph illustrates the nodal characteristics of the FPN following the acupuncture group treatment. The y-axis represents the degree count. where blue bars indicate Out-degree (efferent connections) and red bars indicate In-degree (afferent connections). No specific core regions (hubs) were identified in the acupuncture group after treatment. The L_PCUN, R_IPL and R_SFGmed function as information output nodes. Conversely, the R_PCUN, L_MTG and R_SFGdor serve as information input nodes.

Table 9 ROI1→ROI2 Connections Within the FPN Showing Significant Differences in GCA Values Between the Acupuncture and Drug Groups After Treatment

ROI1			ROI2			T value	*P* value	
Brain Regions	**MNI**	**Voxel**	**Brain Regions**	**MNI**	**Voxel**			**Cohen's d**
Acupuncture group>Drug group								
R_INS	42,-9,-9	22	R_Cerebelum_Crus 1	9,-81,-27	252	2.097	0.048	0.62
R_SFGmed	3,27,45	156	R_Cerebelum_Crus 1	9,-81,-27	252	2.398	0.026	0.71
R_INS	42,-9,-9	22	L_MTG	−63,-39,-9	288	2.506	0.021	0.74
L_PCUN	−6,-72,48	20	L_MTG	−63,-39,-9	288	2.684	0.014	0.79
Acupuncture group<Drug group								
L_Cerebelum_Crus II	−39,-72,-39	50	R_SFGmed	3,27,45	156	−2.097	0.048	0.62
R_Cerebelum_Crus I	9,-81,-27	252	R_INS	42,-9,-9	22	−2.339	0.029	0.69
L_MTG	−63,-39,-9	288	R_SFGdor	33,63,3	1622	−2.172	0.041	0.64
R_ITG	60,-45,-12	189	R_SFGdor	33,63,3	1622	−2.329	0.030	0.69
R_SFGdor	33,63,3	1622	L_Cerebelum_Crus II	−39,-72,-39	50	−2.133	0.045	0.63

At present, treatment efficacy in AD is most commonly assessed using cognitive rating scales in clinical practice. Previous studies have typically evaluated the clinical value of interventions based on whether the change in scale scores before and after treatment reaches statistical significance.[30] However, this approach may overlook the potential practice effect associated with repeated administration of the same assessment, and statistical significance alone does not necessarily imply clinical meaningfulness. The minimal clinically important difference (MCID) refers to the smallest change in an outcome that is perceived as beneficial by patients in the absence of adverse effects or additional burden,

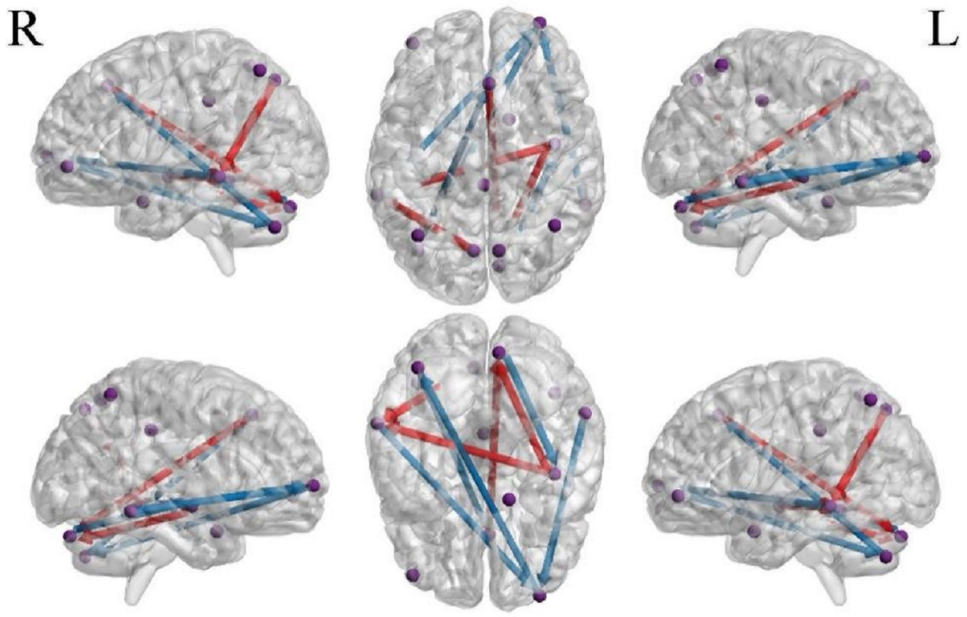

Figure 10 Effective connectivity between ROIs within the FPN showing significant differences in GCA values between the acupuncture and drug groups after treatment. **Note**: Purple spheres represent the regions of interest (ROIs) within the FPN. Arrows denote the directionality of Granger causal influences, indicating significant causal relationships between brain regions (P<0.05). Red lines represent enhanced effective connectivity, while blue lines indicate reduced effective connectivity. The thickness of the lines reflects the magnitude of the increase or decrease in connectivity strength.Between-group comparisons of effective connectivity following treatment. Compared with the drug group, the acupuncture group exhibited significantly higher effective connectivity in the following pathways: R_INS→R_Cerebelum_Crus1, R_SFGmed→R_Cerebelum_Crus1, R_INS→L_MTG, and L_PCUN→L_MTG (P<0.05). Conversely, compared with the acupuncture group, the drug group showed significantly higher effective connectivity in the following pathways: L_Cerebelum_Crus2→R_SFGmed, R_Cerebelum_Crus1→R_INS, L_MTG→R_SFGdor, R_ITG→R_SFGdor, and R_SFGdor→L_Cerebelum_Crus2 (P<0.05).

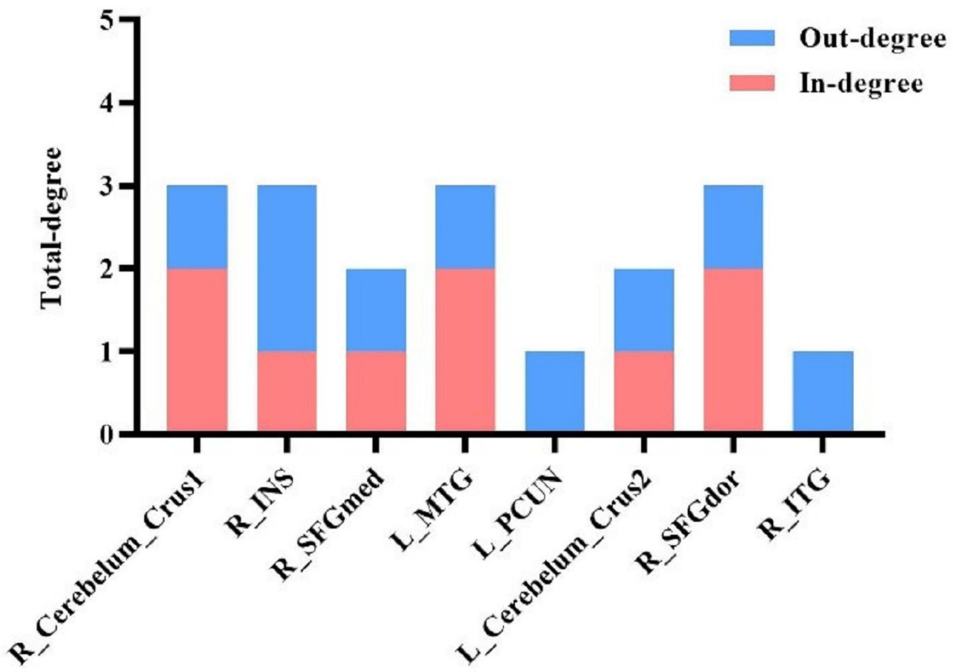

Figure 11 Comparison of total node degree of effective connectivity within the FPN between the acupuncture and drug groups after treatment.
Note: The bar chart illustrates the nodal characteristics of the FPN derived from the between-group comparison.The y-axis represents the degree count. where blue bars indicate Out-degree (efferent connections) and red bars indicate In-degree (afferent connections).No core regions (hubs) were identified based on the total degree threshold. The R_INS functioned as a central source node, whereas the R_Cerebelum_Crus1, L_MTG and R_SFGdor served primarily as central target nodes.

and it is widely regarded as an important indicator of an instrument's responsiveness, namely, its ability to detect a clinically meaningful change.[31,32] Previous literature has suggested that an MCID of at least 2 points on the MoCA represents a clinically meaningful improvement in global cognitive function.[33,34] In the present study, total MoCA-B scores increased significantly after treatment in both the acupuncture and drug groups, and the mean pre- to post-treatment change exceeded 2 points in both groups. These findings suggest that, even after accounting for the potential contribution of practice effects, both treatments may confer meaningful cognitive benefits in patients with AD and therefore possess practical clinical value. Notably, the greater improvement observed in the acupuncture group than in the drug group further suggests that acupuncture combined with western medication may be more effective than western medication alone in improving cognitive function in patients with AD.

To our knowledge, this is one of the few studies to employ bivariate GCA to systematically investigate impairments in effective connectivity within the FPN in AD patients and to explore potential neural mechanisms underlying acupuncture intervention. Previous studies have suggested that reduced functional connectivity reflects regional functional impairment, whereas enhanced connectivity may indicate functional reorganization or compensatory mechanisms.[35] In the present study, compared with the healthy control group, AD patients exhibited decreased GCA values among ROIs located mainly in the parietal and temporal lobes, indicating weakened effective connectivity. In contrast, increased GCA values were observed in ROIs primarily distributed in the frontal and temporal lobes, suggesting enhanced effective connectivity. These findings indicate that, even at rest, the FPN in AD patients exhibits a coexistence of functional suppression, aberrant hyperactivation, and compensatory excitation. Among these regions, the right inferior parietal lobule gyrus and the left middle temporal gyrus were identified as core nodes of the FPN, playing critical roles in information integration and redistribution within the network. Treatment with donepezil alone primarily enhanced effective connectivity between frontal and cerebellar ROIs and parietal ROIs within the FPN. In contrast, combined acupuncture and donepezil treatment significantly strengthened effective connectivity between the bilateral precuneus. Furthermore, post-treatment between-group comparisons revealed that both donepezil and acupuncture modulated effective connectivity between the frontal cortex and cerebellum, as well as between the temporal and frontal cortices. Notably, acupuncture intervention exerted stronger regulatory effects than donepezil on effective

connectivity from frontal regions (right insula and right superior frontal gyrus, medial) to the cerebellum (right cerebellum Crus I), as well as from the frontal cortex (right insula) to the temporal cortex (left middle temporal gyrus). Conversely, donepezil treatment showed greater effects than acupuncture in modulating effective connectivity from the cerebellum (left cerebellum Crus II and right cerebellum Crus I) to frontal regions (right superior frontal gyrus, medial and right insula), and from the temporal cortex (left middle temporal gyrus and right inferior temporal gyrus) to the frontal cortex (right superior frontal gyrus, dorsolateral). In addition, acupuncture intervention demonstrated a stronger regulatory effect than donepezil on effective connectivity from the parietal cortex (left precuneus) to the temporal cortex (left middle temporal gyrus).

Impairment-Related Alterations of Effective Connectivity Within the FPN in Patients with AD

The temporal lobe plays a critical role in memory association, language recognition, and visuospatial information integration, whereas the parietal lobe is closely associated with episodic memory, spatial cognition, calculation, and sensory processing. The temporoparietal region constitutes a complex multimodal area that receives convergent inputs from the thalamic, visual, auditory, somatosensory, and limbic systems, and forms bidirectional connections with distal temporal regions and the prefrontal cortex. This region is therefore deeply involved in the processing of diverse social and cognitive information. In particular, the temporoparietal junction—especially the inferior parietal lobule and posterior temporal cortex—has been regarded as a core hub for multisensory integration and processing.[36] Siok et al[37] reported that functional abnormalities within the temporoparietal region can lead to severe reading impairments. In the present study, compared with healthy controls, patients with AD exhibited reduced effective connectivity between temporal and parietal regions within the FPN. Such disruption may impair the processing and transmission of incoming information, thereby compromising information integration within this region. This mechanism may represent one of the central neural substrates underlying cognitive deficits, including impaired reading ability, observed in patients with AD. Broadhouse et al[38] demonstrated that functional networks within the frontotemporal cortex are closely associated with higher-order executive functions, decision-making, impulse control, and cognitive flexibility. Abnormal decoupling of frontotemporal functional connectivity has been identified as a neural basis for cognitive and emotional processing deficits. In patients with multidomain amnestic mild cognitive impairment and mild AD, marked cortical thinning in the frontal and temporal regions has been observed, accompanied by significantly reduced functional connectivity between temporal gyri and frontal cortices. In contrast, our results showed enhanced effective connectivity between frontal regions (right superior frontal gyrus, medial and left median cingulate and paracingulate gyri) and temporal regions (right inferior temporal gyrus and left middle temporal gyrus) within the FPN in AD patients compared with healthy controls. We speculate that this enhancement may reflect a compensatory mechanism, whereby increased frontotemporal coordination partially offsets inefficient information processing and abnormal directional information transfer resulting from impaired temporoparietal connectivity, thereby helping to maintain the cognitive regulatory functions of the FPN. In addition, the present study found that both the left middle temporal gyrus and the right inferior temporal gyrus exhibited concurrent increases and decreases in GCA values with other frontal and parietal regions, further underscoring the pivotal role of the temporal lobe as a key integrative hub in large-scale cognitive networks.

Core regions within a neural network play a crucial role in maintaining the stability of network architecture and ensuring efficient information integration.[39] The angular gyrus is located at the parieto-occipital junction and contains abundant neural fibers connecting with visual cortical areas. It is considered a typical visuolinguistic hub involved in the integration of perceptual information and, through its connections with language-related regions in the left temporal and frontal lobes, cooperatively coordinates language processing.[40] In particular, the inferior parietal lobule is closely associated with semantic (lexical) processing.[41] The middle temporal gyrus is a major cortical region for semantic storage and also participates in the regulation of early semantic processing. The left middle temporal gyrus is responsible for extracting specific semantic features and forming semantic representations through the integration of multiple semantic attributes.[42] In the present study, bidirectional effective connectivity was observed between the right inferior parietal lobule and the left middle temporal gyrus in patients with AD. However, effective connectivity from the right inferior parietal lobule to the left middle temporal gyrus was enhanced, whereas connectivity from the left middle

temporal gyrus to the right inferior parietal lobule was reduced. These asymmetric bidirectional alterations may reflect two non-mutually exclusive mechanisms. First, functional impairment of the left middle temporal gyrus in AD may weaken its regulatory influence on the right inferior parietal lobule. In response, a compensatory enhancement of effective connectivity from the right inferior parietal lobule to the left middle temporal gyrus may occur, thereby partially preserving semantic encoding, integration, and related processing functions. Second, this anticorrelated bidirectional connectivity pattern may reflect asynchronous information processing and transmission between semantic control regions, representing an intrinsic neural response to language dysfunction in AD. In addition, the reduced GCA values from the left inferior parietal lobule to the right inferior parietal lobule further suggest impairments in semantic information processing, language memory, and retrieval functions in patients with AD.

The frontal lobe is a key brain region involved in the formation of spatial memory, whereas the parietal lobe is responsible for processing spatial features such as location and orientation. Visuospatial information from the external environment is transmitted from the visual cortex to the parietal association cortex for spatial perception processing and subsequently projected to the dorsal prefrontal cortex, where it is encoded to form spatial memory. These processes indicate that the maintenance of normal spatial working memory relies on coordinated interactions between the parietal and frontal lobes.[43] In addition, the middle frontal gyrus, together with specific parietal regions, constitutes a neural network involved in cross-modal information processing and semantic transformation across different sensory modalities. Within this network, the middle frontal gyrus plays a crucial role in identifying and resolving conflicts among semantic representations derived from different sensory channels.[44] The present study demonstrated that, compared with healthy controls, patients with AD exhibited abnormally enhanced effective connectivity from the right inferior parietal lobule to the left medial frontal gyrus, orbital part. This alteration may represent a distinctive neural correlate of spatial memory impairment in AD and further suggests disrupted information exchange within cross-modal sensory networks. Such abnormalities may underlie clinical manifestations of sensory incongruence, such as mismatches between visual and gustatory information, observed in patients with AD.

The anterior cingulate gyrus and paracingulate gyrus are key components of the limbic system and are primarily involved in the processing of emotional information. Li et al[45] demonstrated that patients with AD exhibit a significant decline in memory for negative emotions (such as fear and anxiety), and that the severity of this impairment is positively correlated with atrophy in emotion-related brain regions, including the left middle temporal gyrus and the cingulate cortex. In the present study, patients with AD showed enhanced effective connectivity from the left median cingulate and paracingulate gyri to the left middle temporal gyrus, accompanied by reduced effective connectivity in the reverse direction—from the left middle temporal gyrus to the left median cingulate and paracingulate gyri. These asymmetric alterations suggest disrupted processing of negative emotional stimuli in AD, reflecting both functional impairment in specific brain regions and compensatory effects mediated by spontaneous feedback regulation within the brain. Collectively, these findings indicate that the AD patients included in this study may exhibit varying degrees of impairment in negative emotional memory.

Compared with the healthy control group, patients with AD exhibited significantly weakened effective connectivity from the right inferior parietal lobule to the right cerebellum Crus I. Previous studies have demonstrated extensive fiber connections between the cerebellum and the parietal cortex, prefrontal cortex, and limbic structures such as the hippocampus and amygdala,[46,47] indicating that the cerebellum is closely involved in multidomain cognitive functions and emotional processing. Rice et al[48] reported that the cerebellum plays an important role in normal language regulation, and Nakatani H et al[49] further showed that the right cerebellum Crus I participates in the modulation of multiple language-related tasks. Projections between the cerebellum and cerebral cortex facilitate coordinated language information processing, suggesting that the right cerebellum Crus I may serve as a potential target region for promoting recovery of language function. Accordingly, the present findings suggest that the reduced effective connectivity from the right inferior parietal lobule to the right cerebellum Crus I in AD patients may be closely associated with impairments in language expression. In addition, previous research has shown that cerebellum Crus II is functionally coupled with frontoparietal associative regions, and that cerebellar–cortical connections convey error-related signals to cognitive control networks, thereby improving internal representations of goal-directed behavior through error monitoring and optimization processes.[50] In the present study, reduced effective connectivity from the left medial frontal gyrus, orbital part to the left cerebellum Crus II was observed, suggesting that patients with AD may

have impaired ability to accurately detect and optimize error-related information, ultimately leading to abnormalities in related cognitive performance.

The orbitofrontal cortex is closely associated with the integration and processing of anger-related emotional information and also plays an important role in conflict resolution and the inhibition of aggressive or impulsive behaviors.[51] The superior frontal gyrus, in contrast, is a brain region specialized for the processing of happy prosody —including acoustic features such as pitch and duration during speech production—and is particularly adept at extracting positive emotional prosody from negative emotional contexts, such as fear or anger, under specific task conditions.[52] In the present study, patients with AD exhibited abnormally enhanced effective connectivity from the right inferior frontal gyrus, orbital part to the right superior frontal gyrus, medial. Such alterations may lead to disordered encoding of complex emotional information, thereby impairing normal emotional regulation and social functioning. Clinically, this dysregulation may manifest as increased irritability, impulsivity, or aggressive behaviors in patients with AD.

The inferior temporal gyrus is closely connected with the frontal lobe and memory-related cortices. It is also a key component of the ventral visual pathway, contributing to the integration and relay of visual information. Martinez-Trujillo and J[53] reported that, under attentional control, the ITG is responsible for filtering out information irrelevant to the current goal. The feedback pathway from the frontal cortex to ventral visual regions, including the ITG, provides a structural basis for top–down modulation of selective attention.[54] In the present study, compared with the healthy control group, patients with AD showed increased GCA between the right ITG and the right medial superior frontal gyrus, which may be associated with abnormal selection of task-relevant information elicited by specific visual stimuli and dysregulated attentional control.

Taken together with prior domestic and international evidence and in light of our findings, AD patients exhibit abnormal alterations in effective connectivity within the FPN. Specifically, reduced effective connectivity at parietal hubs, within parieto-temporal regions, between parietal and frontal cortices, and between parietal regions and the cerebellum may primarily contribute to impaired processing and integration of semantic information, thereby resulting in language dysfunction. Increased or decreased fronto-temporal effective connectivity may lead to an imbalance in the interregional exchange and transmission of negative emotional information flow, giving rise to deficits in negative emotional memory. In addition, enhanced local frontal and fronto-parietal effective connectivity is associated with spatial memory decline, disorganized encoding of complex emotional information, and aberrant expression of information across sensory modalities, and may further manifest as impulsive behaviors such as irritability and aggression toward others.

Effects of Donepezil on Effective Connectivity Among FPN-Related Regions in AD Patients

Compared with the healthy control group, AD patients showed a significant increase in effective connectivity within the FPN from the right inferior parietal lobule to the left medial frontal gyrus, orbital part. After treatment in the donepezil, functional connectivity between these two regions was markedly reduced, suggesting that donepezil may ameliorate abnormal frontoparietal coupling within the FPN, help restore normal processing of cross-modal semantic conflict information, and thereby alleviate the clinical manifestations of disordered cross-modal information expression in AD. The medial and paracingulate gyri, together with the superior frontal gyrus, are involved in the processing of emotional information. In this study, the GCA value from the left median cingulate and paracingulate gyri to the right superior frontal gyrus, medial increased significantly after donepezil treatment compared with pre-treatment, indicating that conventional pharmacotherapy may attenuate maladaptive emotional responses in AD. The precuneus, located on the medial parietal lobe, plays a central role in a wide range of cognitive integration tasks. It contributes to the formation of visuospatial imagery and to the encoding and retrieval of spatial location information,[55,56] and is also crucial for emotional-memory processing, self-awareness, and the maintenance of visuospatial representations. Abnormal precuneus function has been linked to negative self-referential cognition, such as unwarranted self-blame and low self-evaluation.[57] The cerebellum receives inputs from multiple regions, including the prefrontal cortex, posterior parietal cortex, and superior temporal gyrus, forming the "cerebro–cerebellar circuit" and participating in the regulation of cognition-related processes such as memory, language, and emotion.[58] Taken together, our findings suggest that conventional

pharmacotherapy may reduce cognitive impairment and adverse emotional responses in AD by strengthening effective connectivity between the cerebrum and cerebellum, thereby facilitating more efficient processing of cognition- and emotion-related information.

Effects of Acupuncture Combined with Donepezil on Effective Connectivity Among FPN-Related Regions in AD Patients

Compared with the healthy control group, combined acupuncture and donepezil treatment was associated with a significant reduction in GCA values from the right inferior parietal lobule gyrus to the left middle temporal gyrus. This finding suggests that the combined therapy may help restore functional impairment in the left middle temporal gyrus and attenuate excessive feedback regulation in the brain, thereby promoting a covarying connectivity pattern between the right inferior parietal lobule and the left middle temporal gyrus. Such a pattern may facilitate normal bidirectional transmission of stimulus-related information across parieto-temporal regions and, in turn, improve language function in AD patients. In addition, AD patients exhibited abnormally increased effective connectivity among local frontal regions. After intervention, the GCA value from the right superior frontal gyrus, medial to the right superior frontal gyrus, dorsolateral was significantly reduced compared with baseline, indicating that acupuncture combined with pharmacotherapy may exert a beneficial bidirectional modulation of altered local frontal functional coordination. A prior *f*MRI study reported that, based on its connectivity with other cortical areas, the precuneus can be subdivided into three subregions: an anterior precuneus (sensorimotor subregion) connected with the cingulate gyrus and supplementary motor area, a central precuneus (cognitive subregion) connected with frontal, parietal, and temporal cortices, and a posterior precuneus (visual subregion) connected with the visual cortex.[59] Our results further showed strengthened causal interactions between the bilateral precuneus after intervention in the Acupuncture group, suggesting that enhanced effective connectivity between the left and right precuneus may be one pathway through which acupuncture combined with donepezil improves multi-domain cognitive function, as well as visual and sensorimotor impairments, in AD patients.

Effects of Acupuncture on Effective Connectivity Among FPN-Related Regions in AD Patients

Based on the between-group comparison (AD group vs. HC group) and the subtraction analysis of post-treatment changes (Acupuncture group vs. Drug group), our findings suggest that a potential neural mechanism of acupuncture for AD involves beneficial modulation of effective connectivity between the frontal lobe and cerebellum, between temporal and frontal regions, and between parietal and temporal regions. Acupuncture not only selectively regulated effective connectivity within the FPN—particularly involving the right insula and the pathway from the left precuneus to the left middle temporal gyrus—but also highlighted the frontal–cerebellar network as a principal target through which acupuncture modulates FPN connectivity in AD.

The frontal lobe is closely associated with working memory, attention, executive function, and emotional expression. Evidence indicates that, under evolutionary pressures, multiple interconnected functional systems in the human brain underwent coordinated evolution; notably, the prefrontal cortex is tightly linked with cerebellum Crus I and Crus II, forming a prefrontal–cerebellar circuit that contributes to the regulation of language production, emotional responses, and working memory.[60] Cerebellum Crus I/II typically receive projections from the prefrontal cortex and surrounding neuronal populations; after integrating incoming information, signals are relayed to the ventral dentate nucleus and then returned to the prefrontal cortex via the dorsal thalamus,[61] supporting the view that the cerebellum is a key region for multi-domain cognitive control. Wang et al[62] demonstrated that cerebellar damage can disrupt the topological organization of cognitive brain networks, impair cerebro–cerebellar circuit function, and lead to deficits in memory, executive function, visuospatial abilities, and language, as well as abnormal emotional responses. Yao et al[63] further reported that 5-Hz repetitive transcranial magnetic stimulation (rTMS) applied to the bilateral cerebellum can effectively modulate intrinsic functional connectivity between the cerebellum and the dorsolateral and medial prefrontal cortices, thereby improving multi-domain cognitive function in AD. Consistent with these observations, our results showed that acupuncture specifically exerted bidirectional modulation of effective connectivity between frontal regions (right insula;

right superior frontal gyrus, medial and right superior frontal gyrus, dorsolateral) and cerebellum regions (right Crus I and left Crus II), suggesting restoration of normal information exchange and integration within the frontal–cerebellar circuit and concomitant alleviation of cognitive and affective disturbances in AD. Node-degree analysis of FPN effective-connectivity regions further indicated that the right cerebellum Crus I, left middle temporal gyrus, and right superior frontal gyrus, dorsolateral emerged as central targets within the FPN after acupuncture, primarily receiving afferent inputs from other regions. In contrast, the right insula appeared to function as a central "source" node, capable of relaying information simultaneously to the right cerebellum Crus I and the left middle temporal gyrus. Functionally, the right cerebellum Crus I and left middle temporal gyrus are implicated in semantic storage and language encoding, whereas the right superior frontal gyrus, dorsolateral is mainly involved in the retrieval and processing of positive affect. The right insula, considered part of the lateral prefrontal system, can be subdivided into anterior and posterior subregions based on structural and functional characteristics: projections from the anterior insula to the dorsolateral prefrontal cortex are more involved in controlling working memory and attention, while the posterior insula receives inputs from parietal, temporal, and occipital cortices and integrates language, emotion, and sensorimotor information.[64] Given that the precuneus is also broadly engaged in cognitive, visual, and sensorimotor regulation, an integrated functional interpretation of these nodes and their information-transfer roles suggests that acupuncture may primarily improve language function and optimize the processing of perceptual information in AD, while also mitigating adverse emotional responses.

Limitations

The sample size and acupuncture intervention duration in the present study were within the scope of an exploratory trial, which may have introduced potential bias. Future studies will build upon these findings by employing larger sample sizes and longer intervention periods (3–6 months) in randomized controlled trials or longitudinal follow-up studies to further investigate the long-term effects of acupuncture on slowing disease progression.

In terms of neural mechanisms, this study utilized GCA to reveal the modulatory effects of acupuncture on effective connectivity within the frontoparietal network in patients with AD, thereby providing potential targets and directions for future research. However, these findings require independent validation in larger cohorts using more stringent multiple-comparison correction methods.

Moreover, it is important to acknowledge the inherent limitations of GCA in resting-state fMRI studies. The fundamental principle of GCA is to infer directional influences between brain regions based on the predictive relationships of time series data; thus, it reflects "effective connectivity" in a statistical sense rather than direct neurophysiological causality. This approach cannot fully eliminate confounding factors such as global cerebral blood flow fluctuations and physiological noise, and therefore the inferred directional connections should not be interpreted as direct neural regulatory pathways. In addition, conventional GCA is based on a linear interaction model, whereas information processing in neural networks involves complex, nonlinear, and dynamic interactions. This linear assumption may not fully capture the intricate dynamics of brain networks, potentially leading to missed detections or misinterpretation of nonlinear regulatory effects. Therefore, future studies may benefit from integrating multimodal neuroimaging techniques (eg., magnetoencephalography [MEG], intracranial electrophysiology), nonlinear causal analysis methods (eg., transfer entropy), and computational modeling to further validate and refine the neural mechanisms identified in the present study.

Conclusion

In summary, this study provides preliminary evidence that the "Yizhi Tiaoshen" acupuncture prescription combined with donepezil hydrochloride yields superior therapeutic benefits for AD compared with pharmacotherapy alone. Resting-state *f*MRI further demonstrated that both conventional medication and acupuncture can ameliorate functional impairment within the FPN and attenuate maladaptive emotional responses in AD patients. Conventional medication appeared to preferentially modulate the synchrony of functional activity among local frontal regions, between the cerebellum and parietal cortex, and between parietal and frontal regions, thereby alleviating disordered cross-modal information expression and negative self-referential processing. In contrast, acupuncture primarily improved effective connectivity within the frontal–cerebellar network, with a particular emphasis on regulating language function, while enhancing the

optimization of incoming information processing. These effects may represent one of the key mechanisms through which acupuncture exerts therapeutic benefits in AD.

Data Sharing Statement

The data that support the findings of this study are available on request from the corresponding author, Xingke Yan, upon reasonable request.

Author Contributions

All authors made a significant contribution to the work reported, whether that is in the conception, study design, execution, acquisition of data, analysis and interpretation, or in all these areas; took part in drafting, revising or critically reviewing the article; gave final approval of the version to be published; have agreed on the journal to which the article has been submitted; and agree to be accountable for all aspects of the work.

Funding

This research was funded by the Open Project of the Research Center of Traditional Chinese Medicine, Gansu Province (No. zyzx-2024-zx09, zyzx-2024-zx03), Gansu Province University Teacher Innovation Fund Project(No.2024A-082), Scientific Research Start-up Fund Project for Introduced Talents of Gansu University of Chinese Medicine (No.2024YJRC-06).

Disclosure

The authors report no conflicts of interest in this work.

References

1. Martinez B, Peplow PV. MicroRNAs as diagnostic and therapeutic tools for Alzheimer's disease: advances and limitations. *Neural Regen Res*. 2019;14(2):242–255. doi:10.4103/1673-5374.244784
2. Chou Y-H, Sundman M, Ton That V, et al. Cortical excitability and plasticity in Alzheimer's disease and mild cognitive impairment: a systematic review and meta-analysis of transcranial magnetic stimulation studies. *Ageing Res Rev*. 2022;79:101660. doi:10.1016/j.arr.2022.101660
3. Kosyreva AM, Sentyabreva AV, Tsvetkov IS, et al. Alzheimer's disease and inflammaging. *Brain Sci*. 2022;12(9):1237. doi:10.3390/brainsci12091237
4. Frankish H, Horton R. Prevention and management of dementia: a priority for public health. *Lancet*. 2017;390(10113):2614–2615. doi:10.1016/S0140-6736(17)31756-7
5. Jia L, Quan M, Fu Y, et al. Dementia in China: epidemiology, clinical management, and research advances. *Lancet Neurol*. 2020;19(1):81–92. doi:10.1016/S1474-4422(19)30290-X
6. Zhao X, Li X. The prevalence of Alzheimer's disease in the Chinese Han population: a meta-analysis. *Neurol Res*. 2020;42(4):291–298. doi:10.1080/01616412.2020.1716467
7. Jia L, Du Y, Chu L, et al. Prevalence, risk factors, and management of dementia and mild cognitive impairment in adults aged 60 years or older in China: a cross-sectional study. *Lancet Public Health*. 2020;5(12):e661–e671. doi:10.1016/S2468-2667(20)30185-7
8. Cui M, Jiang Y, Zhao Q, et al. Metabolomics and incident dementia in older Chinese adults: the Shanghai Aging Study. *Alzheimers Dement*. 2020;16(5):779–788. doi:10.1002/alz.12074
9. Ibrahim MM, Gabr MT. Multitarget therapeutic strategies for Alzheimer's disease. *Neural Regen Res*. 2019;14(3):437–440. doi:10.4103/1673-5374.245463
10. Tanaka S, Honda S, Nakano H, et al. Comparison between group and personal rehabilitation for dementia in a geriatric health service facility: single-blinded randomized controlled study. *Psychogeriatrics*. 2017;17(3):177–185. doi:10.1111/psyg.12212
11. Bergamaschi S, Arcara G, Calza A, et al. One-year repeated cycles of cognitive training (CT) for Alzheimer's disease. *Aging Clin Exp Res*. 2013;25(4):421–426. doi:10.1007/s40520-013-0065-2
12. Padala PR, Padala KP, Lensing SY, et al. Repetitive transcranial magnetic stimulation for apathy in mild cognitive impairment: a double-blind, randomized, sham-controlled, cross-over pilot study. *Psychiatry Res*. 2018;261:312–318. doi:10.1016/j.psychres.2017.12.063
13. Teselink J, Bawa KK, Koo GK, et al. Efficacy of non-invasive brain stimulation on global cognition and neuropsychiatric symptoms in Alzheimer's disease and mild cognitive impairment: a meta-analysis and systematic review. *Ageing Res Rev*. 2021;72:101499. doi:10.1016/j.arr.2021.101499
14. Wang -Y-Y, Yu S-F, Xue H-Y, et al. Effectiveness and safety of acupuncture for the treatment of Alzheimer's disease: a systematic review and meta-analysis. *Front Aging Neurosci*. 2020;12:98. doi:10.3389/fnagi.2020.00098
15. Wu L, Dong Y, Zhu C, Chen Y. Effect and mechanism of acupuncture on Alzheimer's disease: a review. *Front Aging Neurosci*. 2023;15:1035376. doi:10.3389/fnagi.2023.1035376
16. Smitha KA, Akhil Raja K, Arun KM, et al. Resting state *f*MRI: a review on methods in resting state connectivity analysis and resting state networks. *Neuroradiol J*. 2017;30(4):305–317. doi:10.1177/1971400917697342
17. Dennis EL, Thompson PM. Functional brain connectivity using *f*MRI in aging and Alzheimer's disease. *Neuropsychol Rev*. 2014;24(1):49–62. doi:10.1007/s11065-014-9249-6

18. Dixon ML, De La Vega A, Mills C, et al. Heterogeneity within the frontoparietal control network and its relationship to the default and dorsal attention networks. *Proc Natl Acad Sci USA*. 2018;115E1598–E1607.
19. Stickland R, Allen M, Magazzini L, et al. Neurovascular coupling during visual stimulation in multiple sclerosis: a MEG-*f*MRI study. *Neuroscience*. 2019;403:54–69. doi:10.1016/j.neuroscience.2018.03.018
20. Paquette T, Jeffrey-Gauthier R, Leblond H, Piché M. Functional neuroimaging of nociceptive and pain-related activity in the spinal cord and brain: insights from neurovascular coupling studies. *Anat Rec*. 2018;301(9):1585–1595. doi:10.1002/ar.23854
21. Kosten L, Emmi SA, Missault S, Keliris GA. Combining magnetic resonance imaging with readout and/or perturbation of neural activity in animal models: advantages and pitfalls. *Front Neurosci*. 2022;16:938665. doi:10.3389/fnins.2022.938665
22. Deshpande G, LaConte S, James GA, et al. Multivariate Granger causality analysis of *f*MRI data. *Hum Brain Mapp*. 2009;30(4):1361–1373. doi:10.1002/hbm.20606
23. Hu Q, Wang Q, Li Y, et al. Intrinsic brain activity alterations in patients with mild cognitive impairment-to-normal reversion: a resting-state functional magnetic resonance imaging study from voxel to whole-brain level. *Front Aging Neurosci*. 2022;13:788765. doi:10.3389/fnagi.2021.788765
24. Wang L, Zhu R, Zhou X, et al. Altered local and remote functional connectivity in mild Alzheimer's disease patients with sleep disturbances. *Front Aging Neurosci*. 2023;15:1269582. doi:10.3389/fnagi.2023.1269582
25. Zhao X, Liu Y, Wang X, et al. Disrupted small-world brain networks in moderate Alzheimer's disease: a resting-state fMRI study. *PLoS One*. 2012;7(3):e33540. doi:10.1371/journal.pone.0033540
26. The Writing Group of the Guidelines for Dementia and Cognitive Impairment in China. Professional committee for cognitive impairment diseases of the neurologist branch of the chinese medical doctor association. Guidelines for the diagnosis and treatment of dementia and cognitive impairment in China (Part II): guidelines for the diagnosis and treatment of Alzheimer's disease in 2018. *Natl Med J China*. 2018;98:971–977.
27. General Administration of Quality Supervision Inspection and Quarantine of China; Standardization Administration of China. *Nomenclature and Location of Acupuncture Points: GB/T 12346-2006*. Beijing: Standards Press of China; 2006.
28. Weintraub S, Besser L, Dodge HH, et al. Version 3 of the Alzheimer disease centers' neuropsychological test battery in the uniform data set (UDS). *Alzheimer Dis Assoc Disord*. 2018;32(1):10–17. doi:10.1097/WAD.0000000000000223
29. Zhan Y, Fu Q, Pei J, et al. Modulation of brain activity and functional connectivity by acupuncture combined with donepezil on mild-to-moderate Alzheimer's disease: a neuroimaging pilot study. *Front Neurol*. 2022;13:912923. doi:10.3389/fneur.2022.912923
30. Kim J-H, Cho M-R, Park G-C, et al. Effects of different acupuncture treatment methods on mild cognitive impairment: a study protocol for a randomized controlled trial[J]. *Trials*. 2019;20(1):551. doi:10.1186/s13063-019-3670-3
31. Guyatt G, Walter S, Norman G. Measuring change over time: assessing the usefulness of evaluative instruments[J]. *J Chronic Dis*. 1987;40(2):171–178. doi:10.1016/0021-9681(87)90069-5
32. Jaeschke R, Singer J, Guyatt GH. Measurement of health status. Ascertaining the minimal clinically important difference[J]. *Control Clin Trials*. 1989;10(4):407–415. doi:10.1016/0197-2456(89)90005-6
33. Wong GKC, Mak JSY, Wong A, et al. Minimum clinically important difference of montreal cognitive assessment in aneurysmal subarachnoid hemorrhage patients. *J Clin Neurosci*. 2017;46:41–44. doi:10.1016/j.jocn.2017.08.039
34. Wu C-Y, Hung S-J, Lin K-C, et al. Responsiveness, minimal clinically important difference, and validity of the MoCA in stroke rehabilitation. *Occupat Therapy Int*. 2019;2019:2517658. doi:10.1155/2019/2517658
35. Zhang Y, Li K, Ren Y, et al. Acupuncture modulates the functional connectivity of the default mode network in stroke patients. *Evid Based Complement Alternat Med*. 2014;2014(1):765413. doi:10.1155/2014/765413
36. Decety J, Lamm C. The role of the right temporoparietal junction in social interaction: how low-level computational processes contribute to meta-cognition. *Neuroscientist*. 2007;13(6):580–593. doi:10.1177/1073858407304654
37. Siok WT, Niu Z, Jin Z, et al. A structural–functional basis for dyslexia in the cortex of Chinese readers. *Proc Natl Acad Sci U S A*. 2008;105(14):5561–5566. doi:10.1073/pnas.0801750105
38. Broadhouse KM, Winks NJ, Summers MJ. Fronto-temporal functional disconnection precedes hippocampal atrophy in clinically confirmed multi-domain amnestic Mild Cognitive Impairment. *EXCLI J*. 2021;20:1458–1473. doi:10.17179/excli2021-4191
39. van den Heuvel MP, Sporns O. Rich-club organization of the human connectome. *J Neurosci*. 2011;31(44):15775–15786. doi:10.1523/JNEUROSCI.3539-11.2011
40. Gray O, Fry L, Montaldi D. Information content best characterises the hemispheric selectivity of the inferior parietal lobe: a meta-analysis. *Sci Rep*. 2020;10(1):15112. doi:10.1038/s41598-020-72228-8
41. Graves WW, Purcell J, Rothlein D, et al. Correspondence between cognitive and neural representations for phonology, orthography, and semantics in supramarginal compared to angular gyrus. *Brain Struct Funct*. 2023;228(1):255–271. doi:10.1007/s00429-022-02590-y
42. Liuzzi AG, Aglinskas A, Fairhall SL. General and feature-based semantic representations in the semantic network. *Sci Rep*. 2020;10(1):8931. doi:10.1038/s41598-020-65906-0
43. Santo-Angles A, Temudo A, Babushkin V, Sreenivasan KK. Effective connectivity of working memory performance: a DCM study of MEG data. *Front Hum Neurosci*. 2024;18:1339728. doi:10.3389/fnhum.2024.1339728
44. Schneider TR, Lorenz S, Senkowski D, Engel AK. Gamma-band activity as a signature for cross-modal priming of auditory object recognition by active haptic exploration. *J Neurosci*. 2011;31(7):2502–2510. doi:10.1523/JNEUROSCI.6447-09.2011
45. Li XS, Wang HB, Yu YQ, et al. Changes in gray matter volume related to emotional memory in Alzheimer's disease. *Chin J Med Imaging Technol*. 2016;32:1015–1019.
46. Zhang P, Duan L, Ou Y, et al. The cerebellum and cognitive neural networks. *Front Hum Neurosci*. 2023;17:1197459. doi:10.3389/fnhum.2023.1197459
47. De Benedictis A, Rossi-Espagnet MC, de Palma L, et al. Networking of the human cerebellum: from anatomo-functional development to neurosurgical implications. *Front Neurol*. 2022;13:806298. doi:10.3389/fneur.2022.806298
48. Rice LC, D'Mello AM, Stoodley CJ. Differential behavioral and neural effects of regional cerebellar tDCS. *Neuroscience*. 2021;462:288–302. doi:10.1016/j.neuroscience.2021.03.008
49. Nakatani H, Nakamura Y, Okanoya K. Respective involvement of the right cerebellar crus I and II in syntactic and semantic processing for comprehension of language. *Cerebellum*. 2022;22(4):739–755. doi:10.1007/s12311-022-01451-y

50. Hwang K, Hallquist MN, Luna B. The development of hub architecture in the human functional brain Network. *Cereb Cortex*. 2013;23 (10):2380–2393. doi:10.1093/cercor/bhs227
51. Beyer F, Münte TF, Göttlich M, Krämer UM. Orbitofrontal cortex reactivity to angry facial expression in a social interaction correlates with aggressive behavior. *Cereb Cortex*. 2015;25(9):3057–3063. doi:10.1093/cercor/bhu101
52. Lei Z, Bi R, Mo LC, et al. The brain mechanism of explicit and implicit processing of emotional prosodies: an fNIRS study. *Acta Psychologica Sinica*. 2021;53(1):15–25. doi:10.3724/SP.J.1041.2021.00015
53. Martinez-Trujillo J. Visual attention in the prefrontal cortex. *Annu Rev Vis Sci*. 2022;8(1):407–425. doi:10.1146/annurev-vision-100720-031711
54. Rolls ET, Deco G, Huang -C-C, et al. Prefrontal and somatosensory-motor cortex effective connectivity in humans. *Cereb Cortex*. 2023;33 (8):4939–4963. doi:10.1093/cercor/bhac391
55. Dadario NB, Sughrue ME. The functional role of the precuneus. *Brain*. 2023;146(9):3598–3607. doi:10.1093/brain/awad181
56. Tanglay O, Young IM, Dadario NB, et al. Anatomy and white-matter connections of the precuneus. *Brain Imaging Behav*. 2022;16(2):574–586. doi:10.1007/s11682-021-00529-1
57. Kawakami S, Okada N, Satomura Y, et al. Frontal pole–precuneus connectivity and depression severity. *Cereb Cortex*. 2024;34:bhae284.
58. Mannarelli D, Pauletti C, Missori P, et al. Cerebellum's contribution to attention, executive functions and timing: psychophysiological evidence from event-related potentials. *Brain Sci*. 2023;13(12):1683. doi:10.3390/brainsci13121683
59. Mailo J, Tang-Wai R. Insight into the precuneus: a novel seizure semiology in a child with epilepsy arising from the right posterior precuneus. *Epileptic Disord*. 2015;17(3):321–327. doi:10.1684/epd.2015.0759
60. Balsters JH, Cussans E, Diedrichsen J, et al. Evolution of the cerebellar cortex: the selective expansion of prefrontal-projecting cerebellar lobules. *Neuroimage*. 2010;49(3):2045–2052. doi:10.1016/j.neuroimage.2009.10.045
61. Ou S-Q, Wei P-H, Fan X-T, et al. Delineating the decussating dentato-rubro-thalamic tract and its connections in humans using diffusion spectrum imaging techniques. *Cerebellum*. 2022;21(1):101–115. doi:10.1007/s12311-021-01283-2
62. Wang D, Yao Q, Yu M, et al. Topological disruption of structural brain networks in patients with cognitive impairment following cerebellar infarction. *Front Neurol*. 2019;10:759. doi:10.3389/fneur.2019.00759
63. Yao Q, Tang F, Wang Y, et al. Effect of cerebellum stimulation on cognitive recovery in patients with Alzheimer disease: a randomized clinical trial. *Brain Stimul*. 2022;15(4):910–920. doi:10.1016/j.brs.2022.06.004
64. Molnar-Szakacs I, Uddin LQ. Anterior insula as a gatekeeper of executive control. *Neurosci Biobehav Rev*. 2022;139:104736. doi:10.1016/j.neubiorev.2022.104736